Single Crystal Diffuse Scattering

Ray Osborn

Neutron and X-ray Scattering Group
Materials Science Division
Argonne National Laboratory

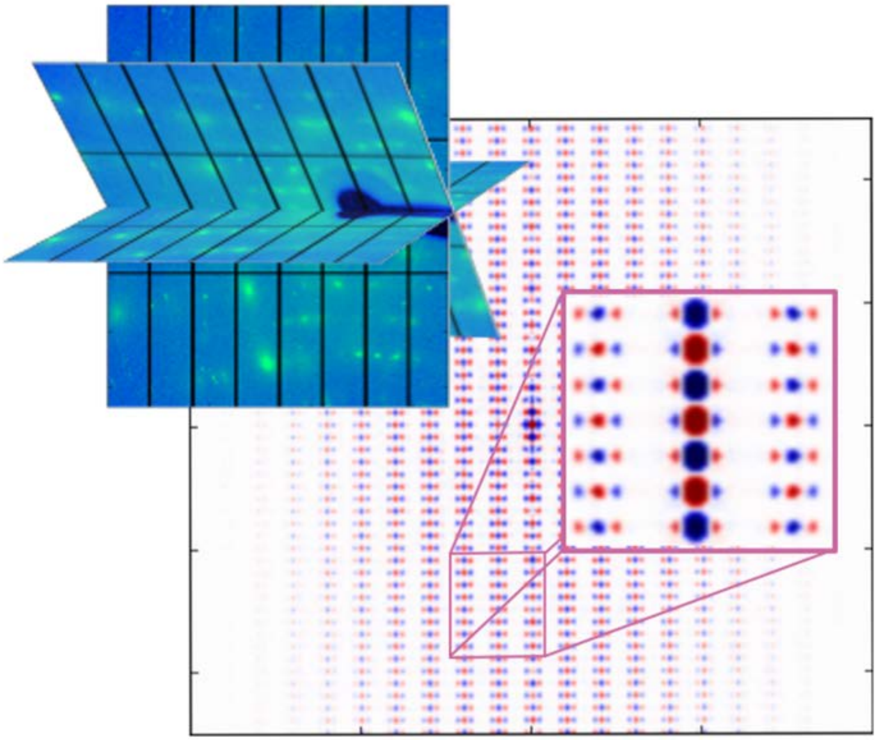

Outline

- What is diffuse scattering?
  - What does it look like?
  - What causes it?
  - Who started it?
- What is it good for?
  - A random walk through disordered materials
- How do I model it?
  - A few equations
  - Rules of thumb
- Case Study 1: Diffuse scattering from vacancies in mullite
- Case Study 2: 3D-ΔPDF in sodium-intercalated V_2O_5
- How do I look at static disorder? *Hint: Corelli*
  - Neutrons *vs* X-rays
  - Diffuse scattering with elastic discrimination
- Diffuse scattering - the musical

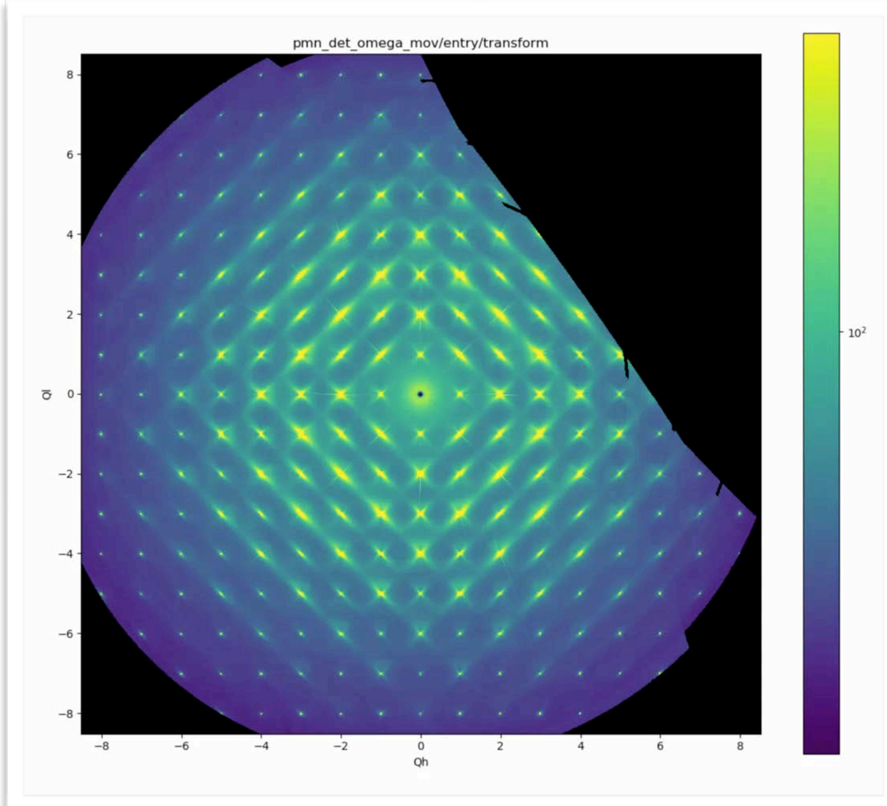

Diffuse Scattering

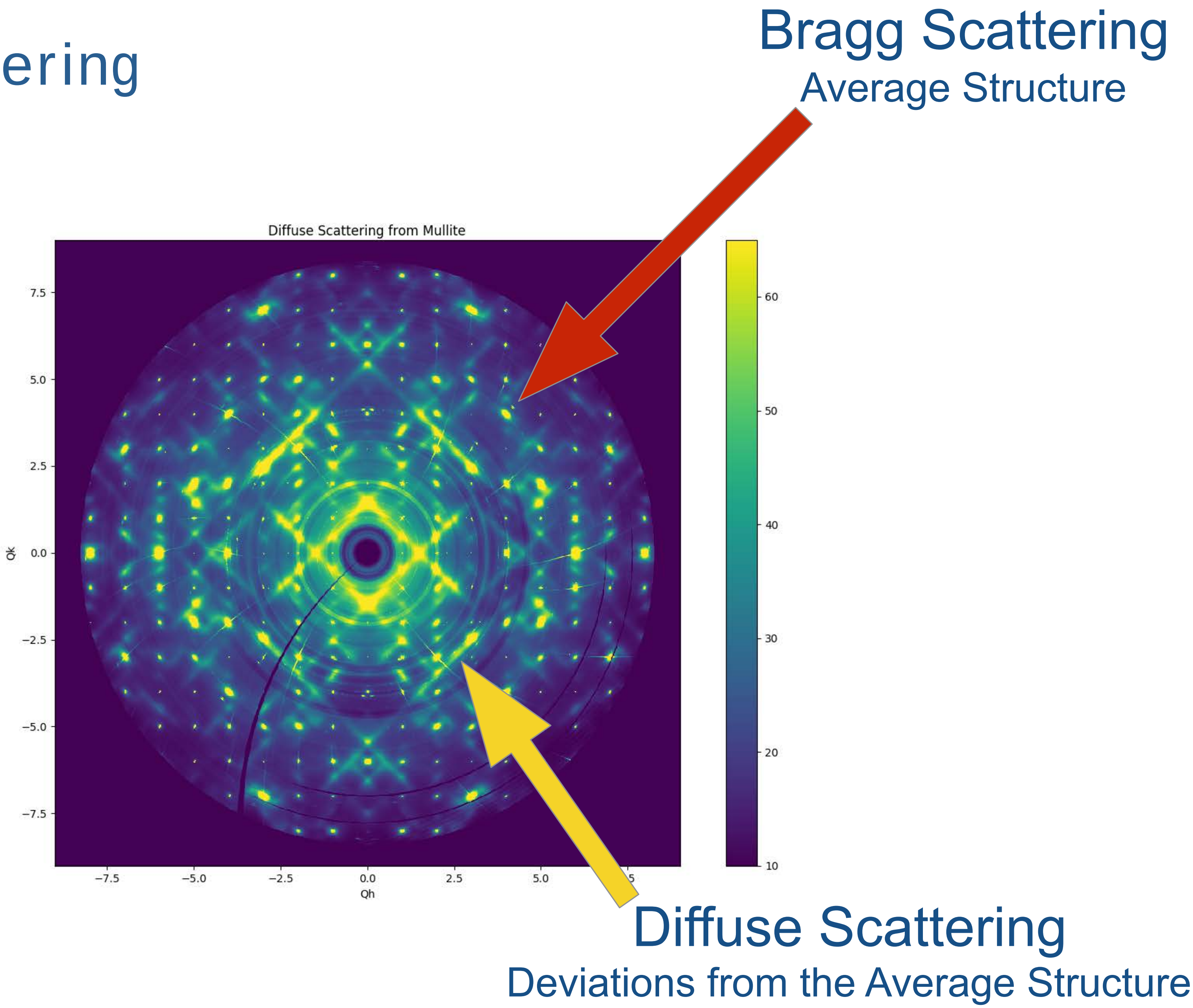

Single Crystal Diffuse Scattering in 3D

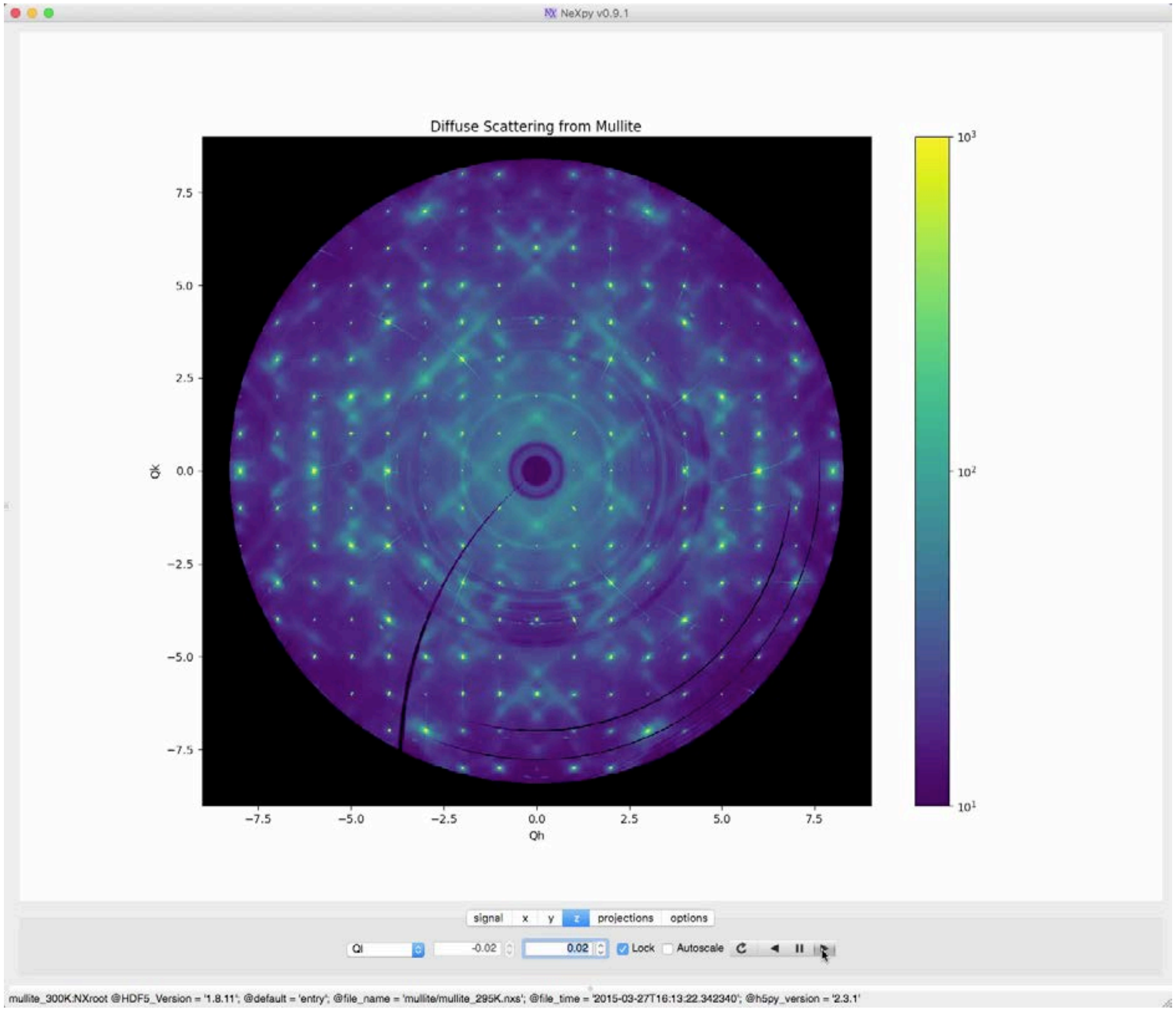

Simple Example of Disorder

- In these examples, 30% of atoms (blue dots) have been replaced by vacancies (green dots)
  - Left-Hand-Side: random substitution
  - Right-Hand-Side: high probability of vacancy clusters
    - Thanks to Thomas Proffen

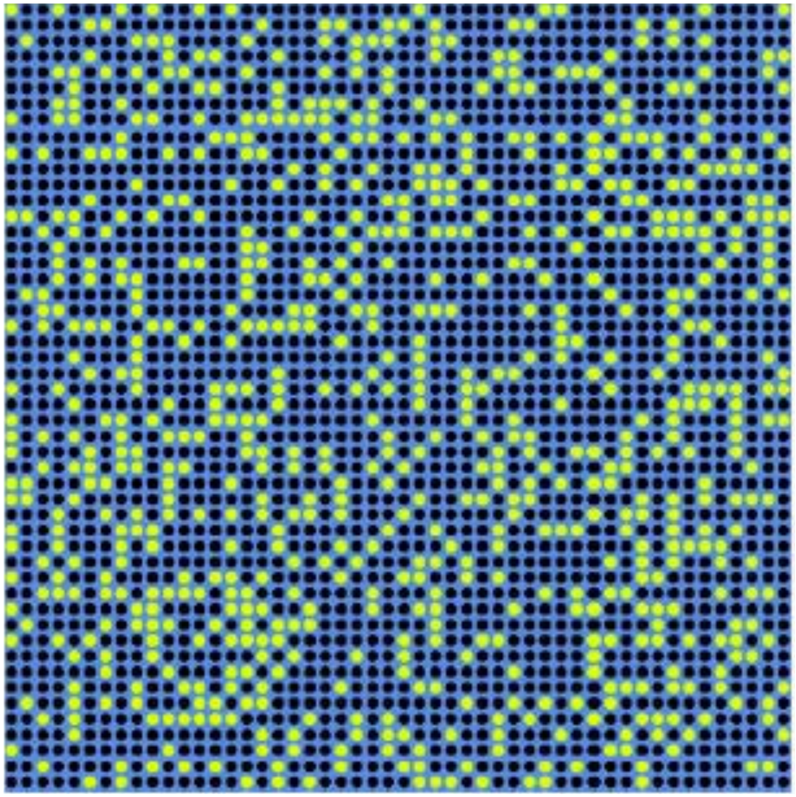

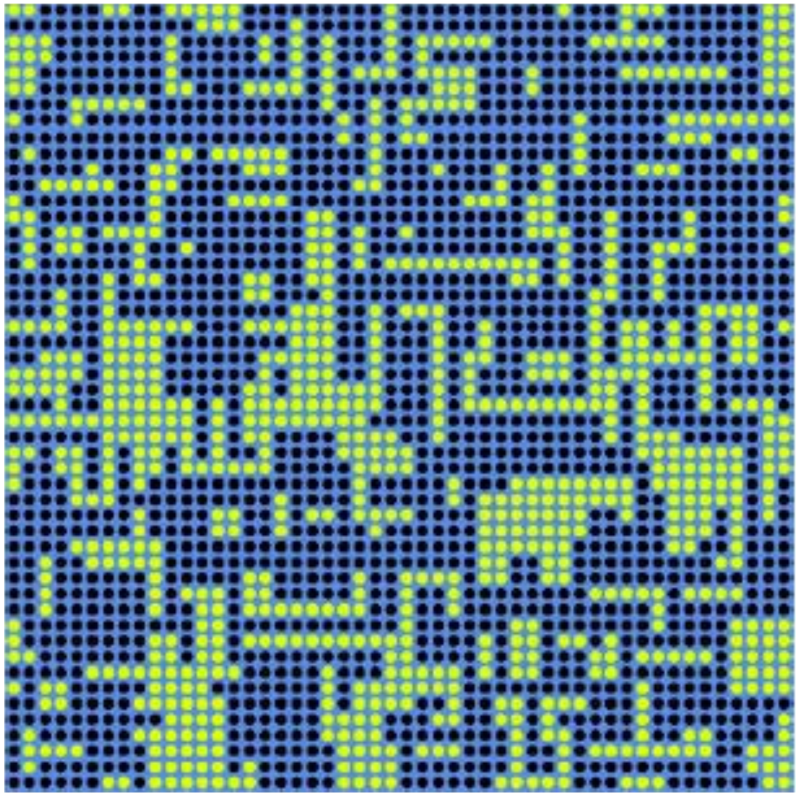

Bragg Scattering

- Bragg scattering is determined by the average structure.
  - Since the average vacancy occupation is identical, both examples have identical Bragg peaks

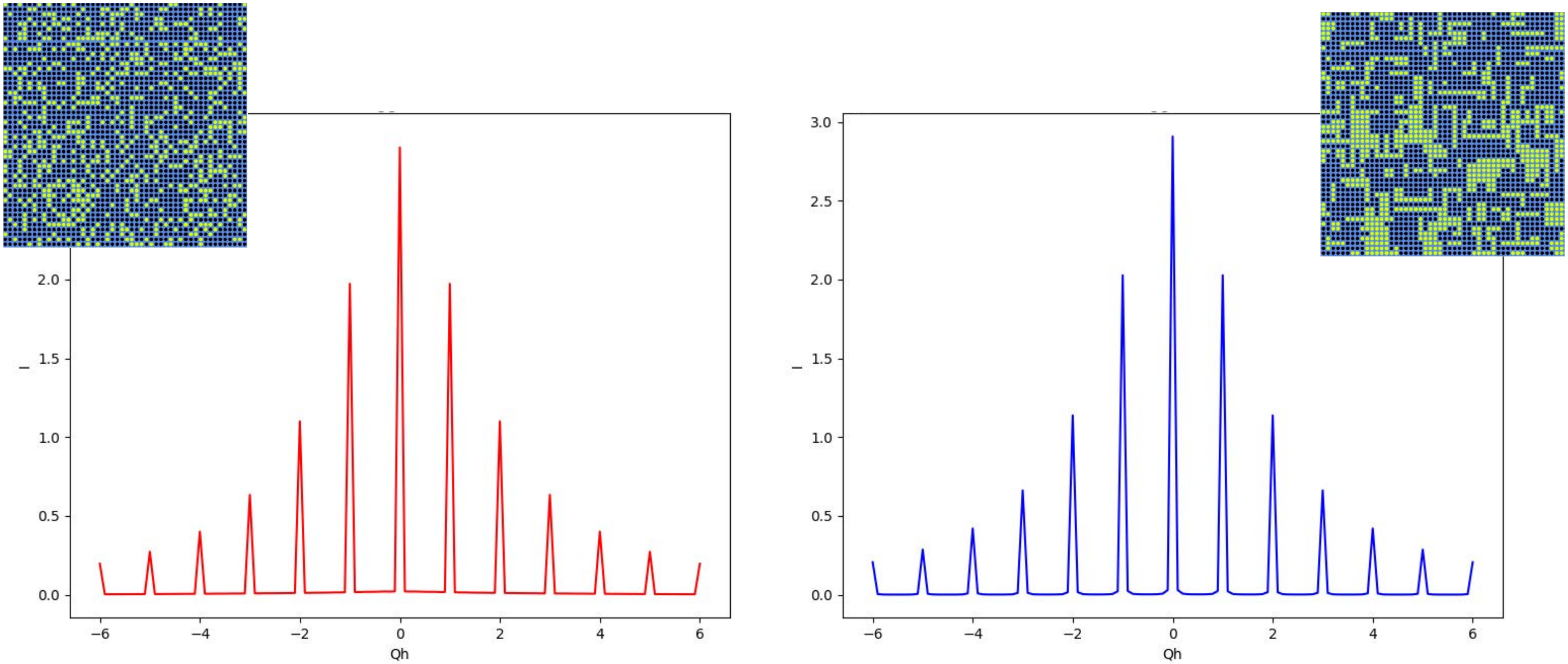

Diffuse Scattering

- The diffuse scattering is quite different in the two examples
  - Random vacancy distributions lead to a constant background (Laue monotonic scattering)
  - Vacancy clusters produce rods of diffuse scattering connecting the Bragg peaks

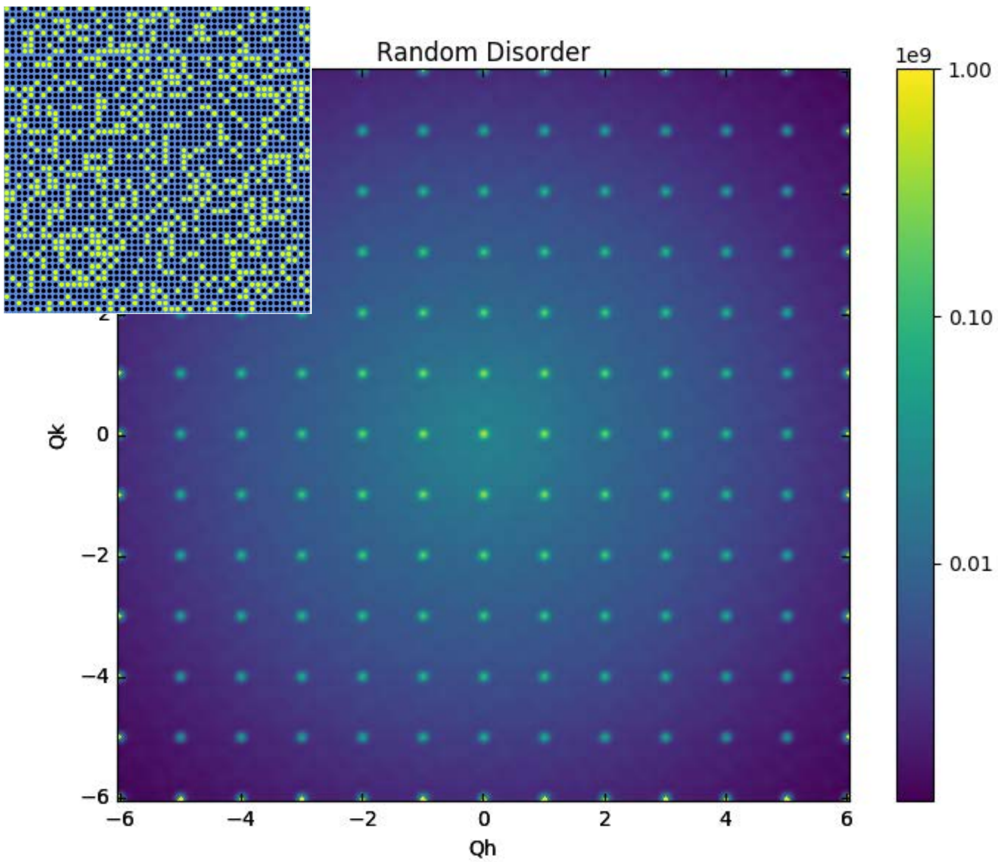

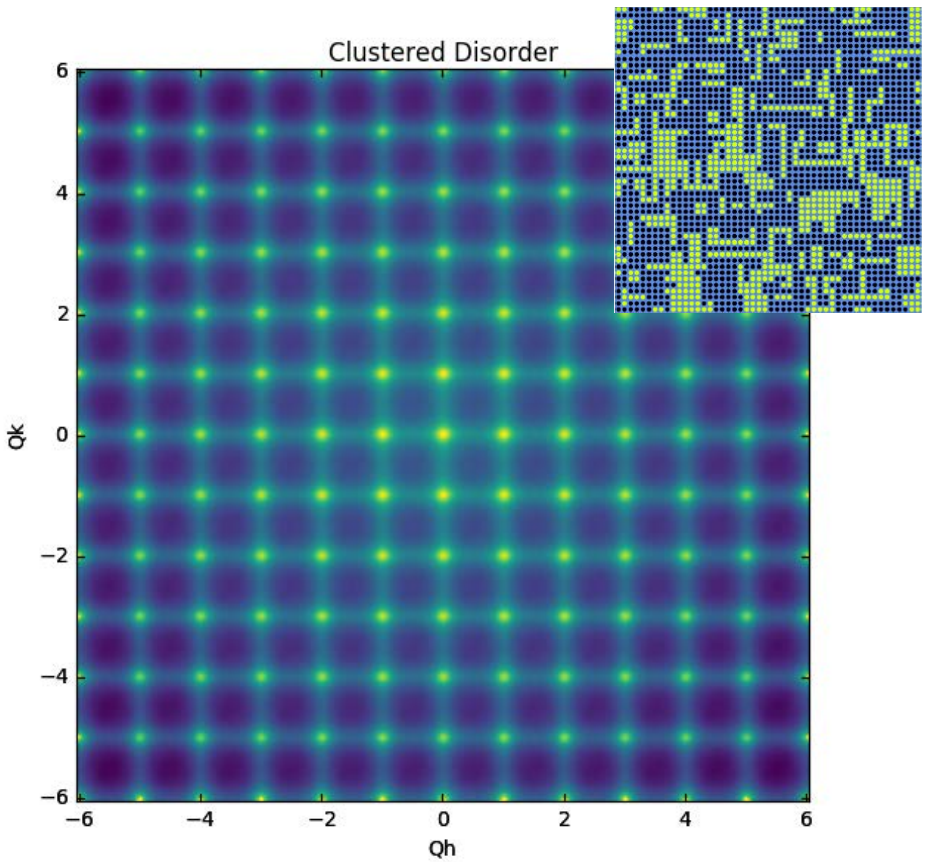

An Ultra-Short History of Advances in Diffuse Scattering

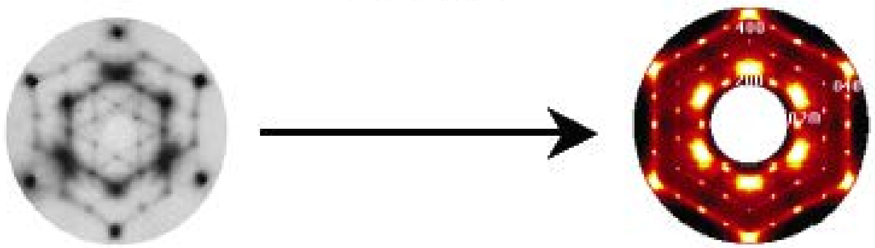

1941 BENZIL 2001

Yttria-Stabilized Zirconia

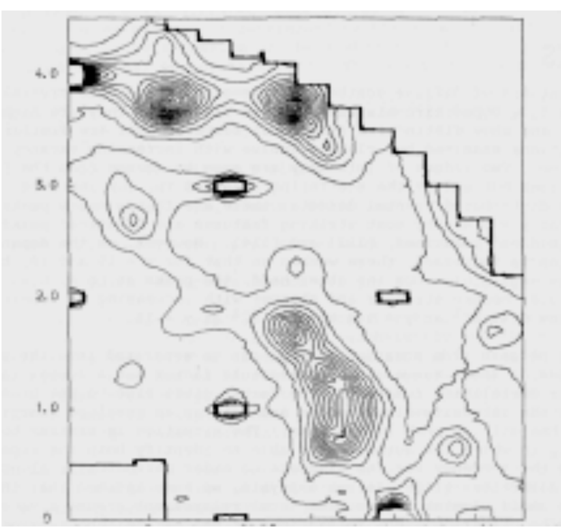

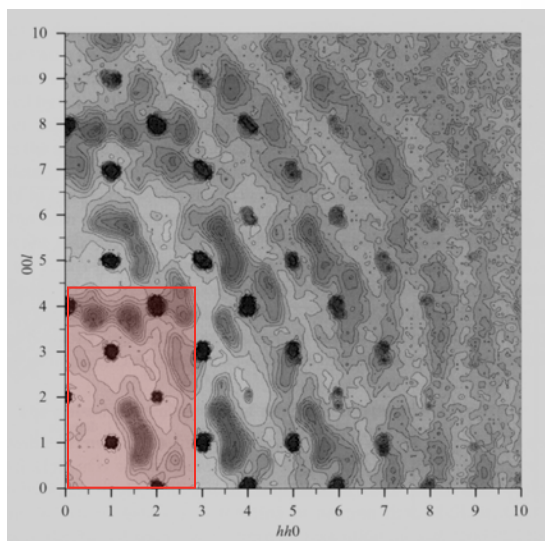

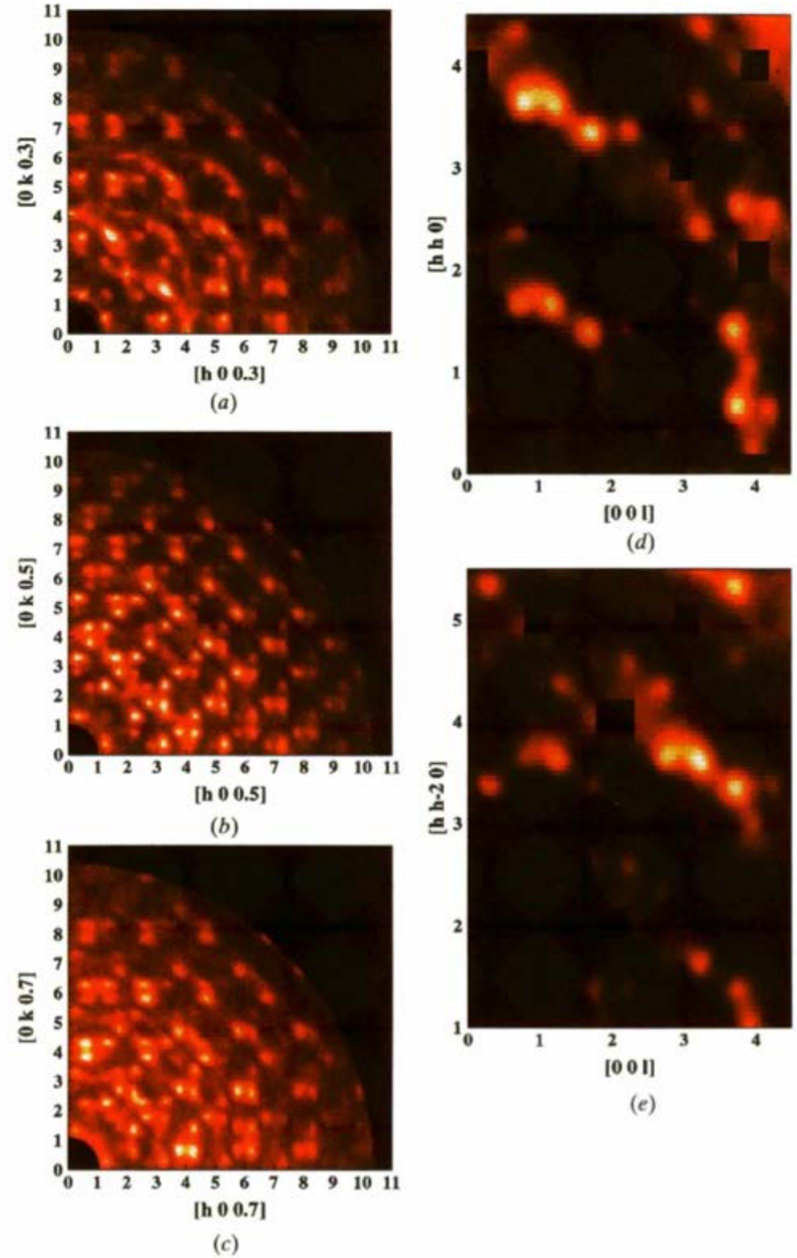

T. Proffen and T. R. Welberry J. Appl. Cryst. **31**, 318 (1998)

What is it good for?

Science Impacted by Diffuse Scattering

- Subjects identified at the *Workshop on Single Crystal Diffuse Scattering at Pulsed Neutron Sources*
  - Stripes in cuprate superconductors
  - Orbital correlations in transition metal oxides (including CMR)
  - Nanodomains in relaxor ferroelectrics
  - Defect correlations in fast-ion conductors
  - Geometrically frustrated systems
  - Critical fluctuations at quantum phase transitions
  - Orientational disorder in molecular crystals
  - Rigid unit modes in framework structures
  - Quasicrystals
  - Atomic and magnetic defects in metallic alloys
  - Molecular magnets
  - Defect correlations in doped semiconductors
  - Microporous and mesoporous compounds
  - Host-guest systems
  - Hydrogen-bearing materials
  - Soft matter - protein configurational disorder using polarization analysis of spin-incoherence
  - Low-dimensional systems
  - Intercalates
  - Structural phase transitions in geological materials

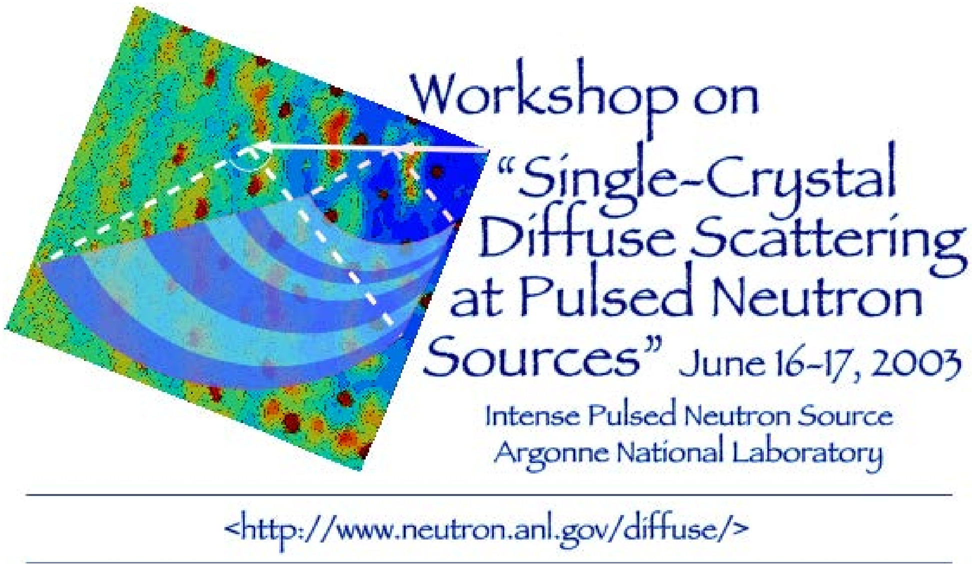

Diffuse Scattering from Metallic Alloys

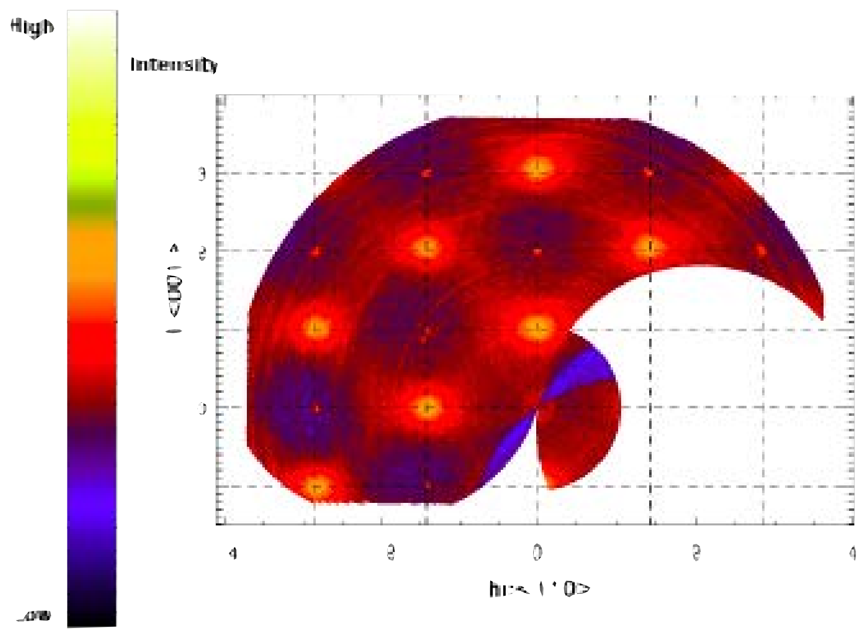

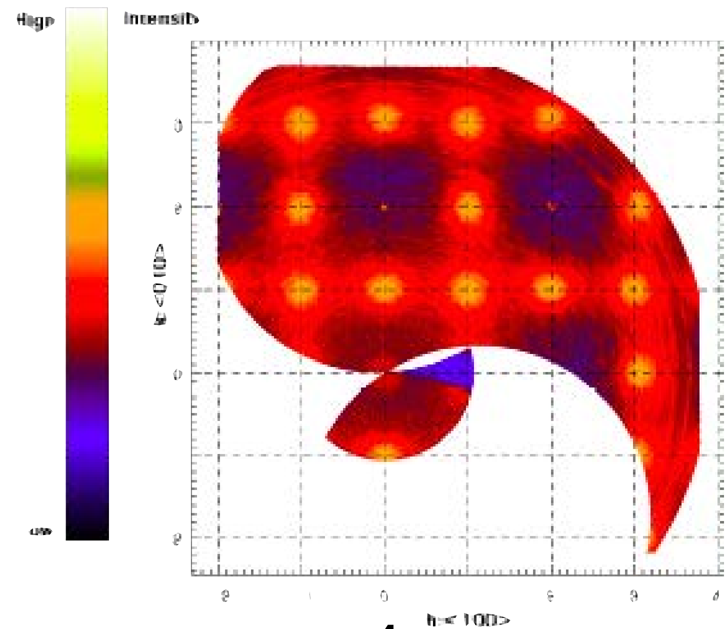

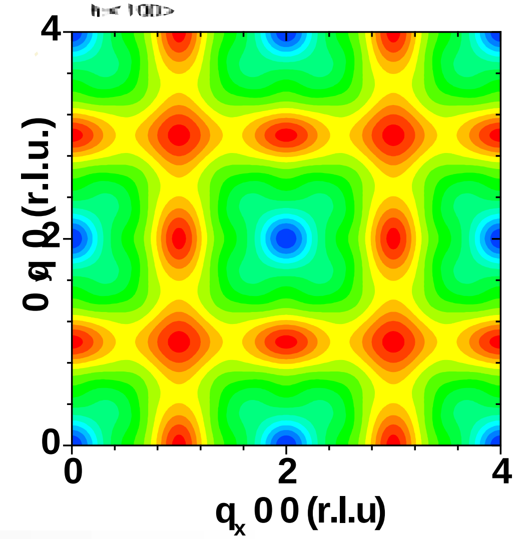

Short-range Order in Null Matrix $^{62}Ni_{0.52}Pt_{0.52}$

J. A. Rodriguez, S. C. Moss, J. L. Robertson, J. R. D. Copley, D. A. Neumann, and J. Major
Phys. Rev. B **74**, 104115

Diffuse Scattering from a Fast-Ion Conductor

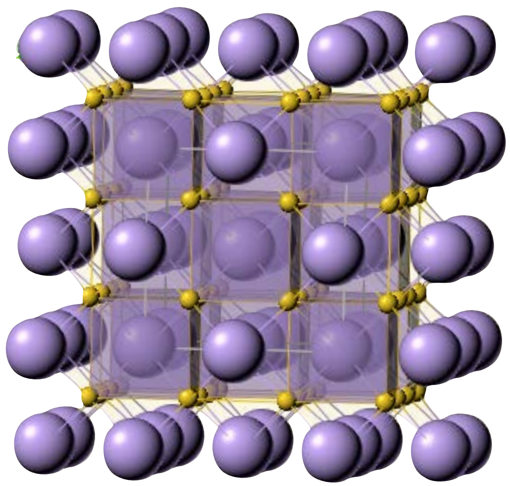

CaF_2

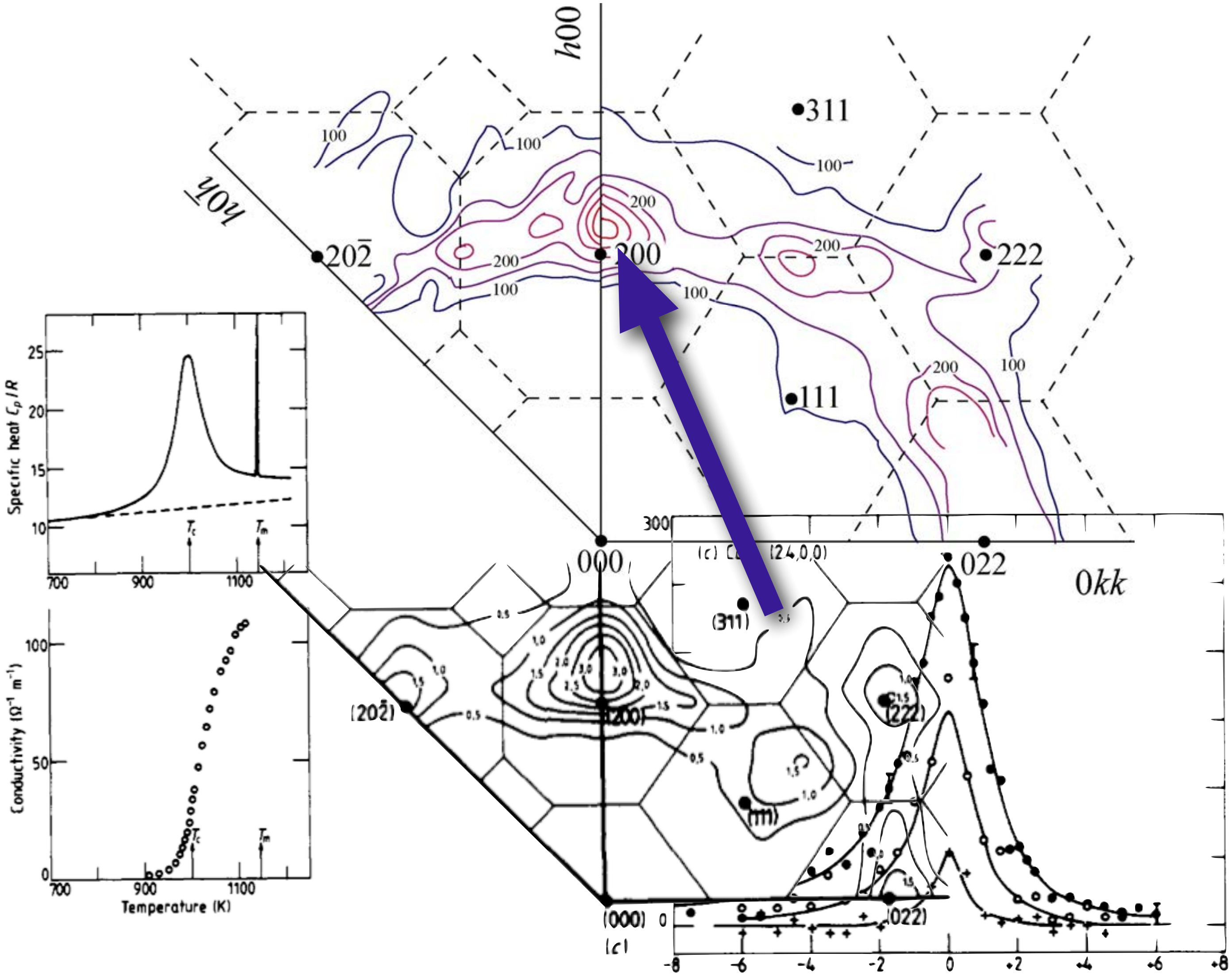

M. T. Hutchings *et al* J. Phys. C **17**, 3903 (1984)

Diffuse Scattering from Molecular Solids

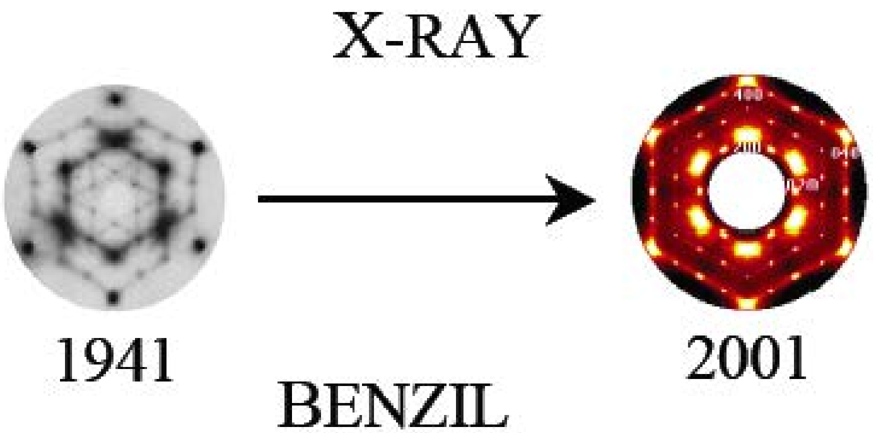

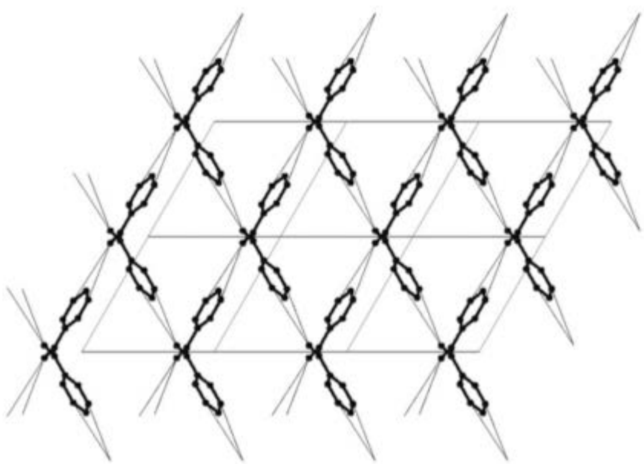

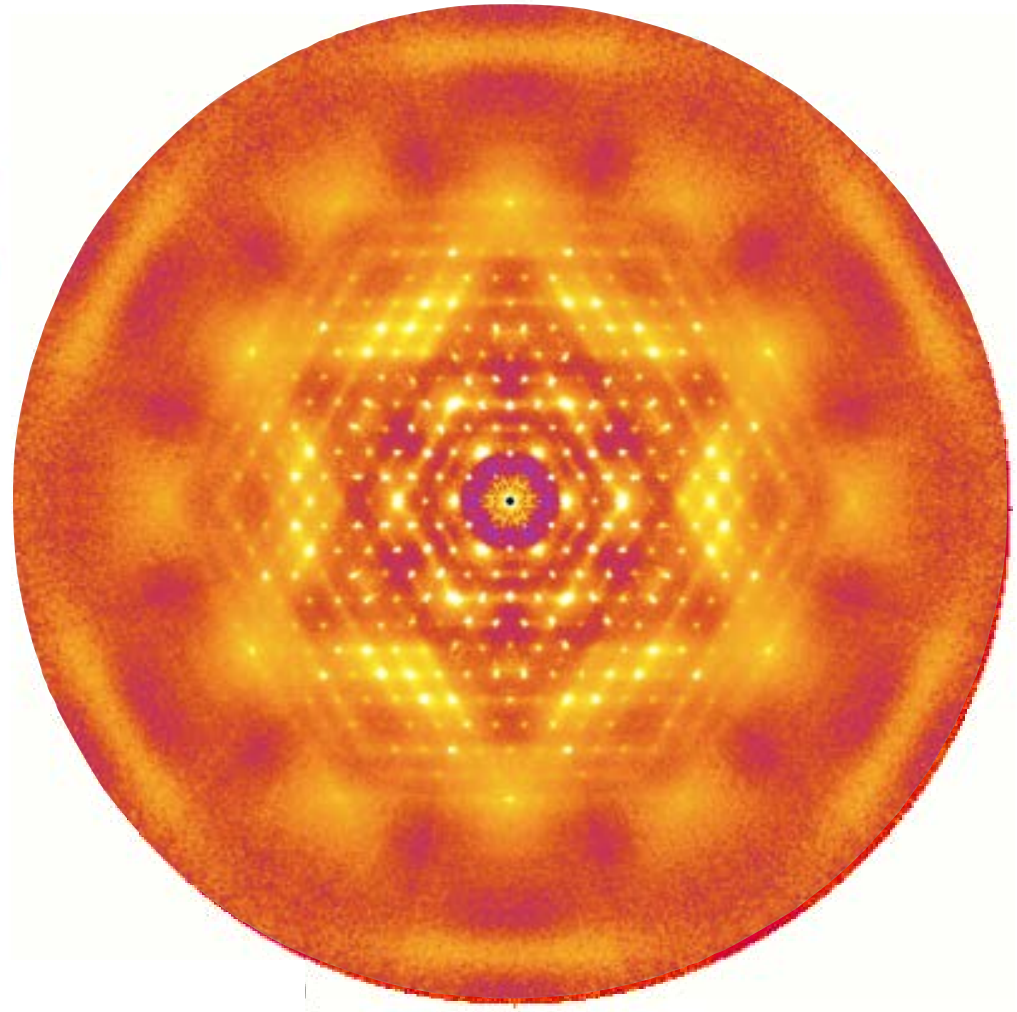

T. R. Welberry *et al* J. Appl. Cryst. **36**, 1400 (2003)

Diffuse Scattering from Relaxor Ferroelectrics

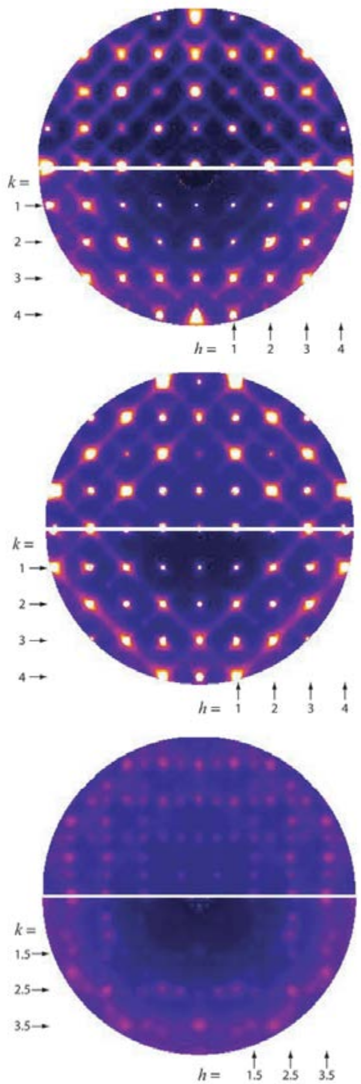

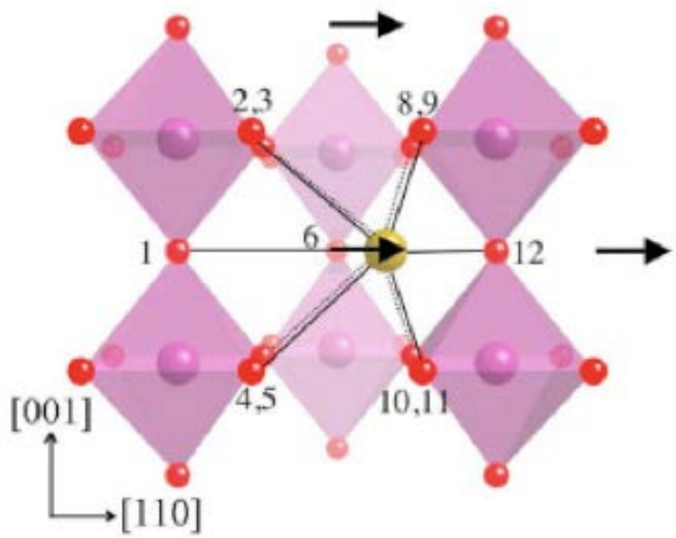

Lead Magnesium-Niobate

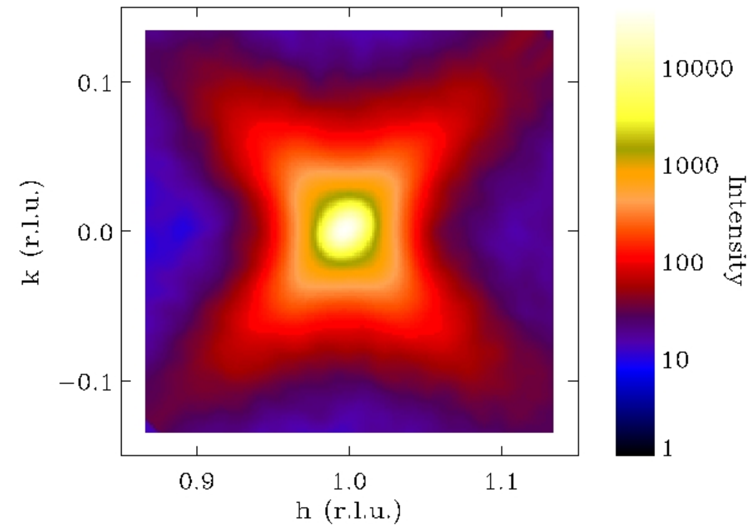

Lead Zinc-Niobate

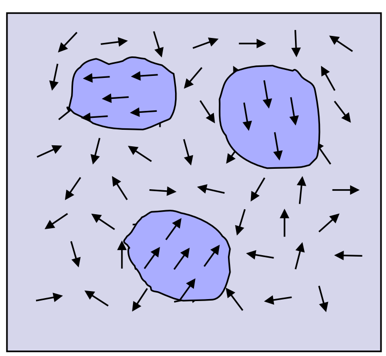

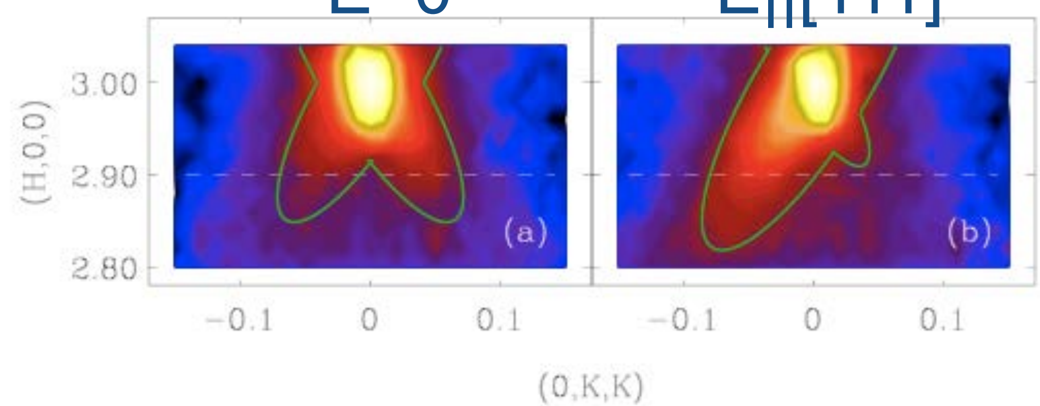

T. R. Welberry *et al* J. Appl. Cryst. **38**, 639 (2005)

G. Xu, P. M. Gehring, G. Shirane, Phys. Rev. B **72**, 214106 (2005).

Diffuse Scattering from Jahn-Teller Polarons

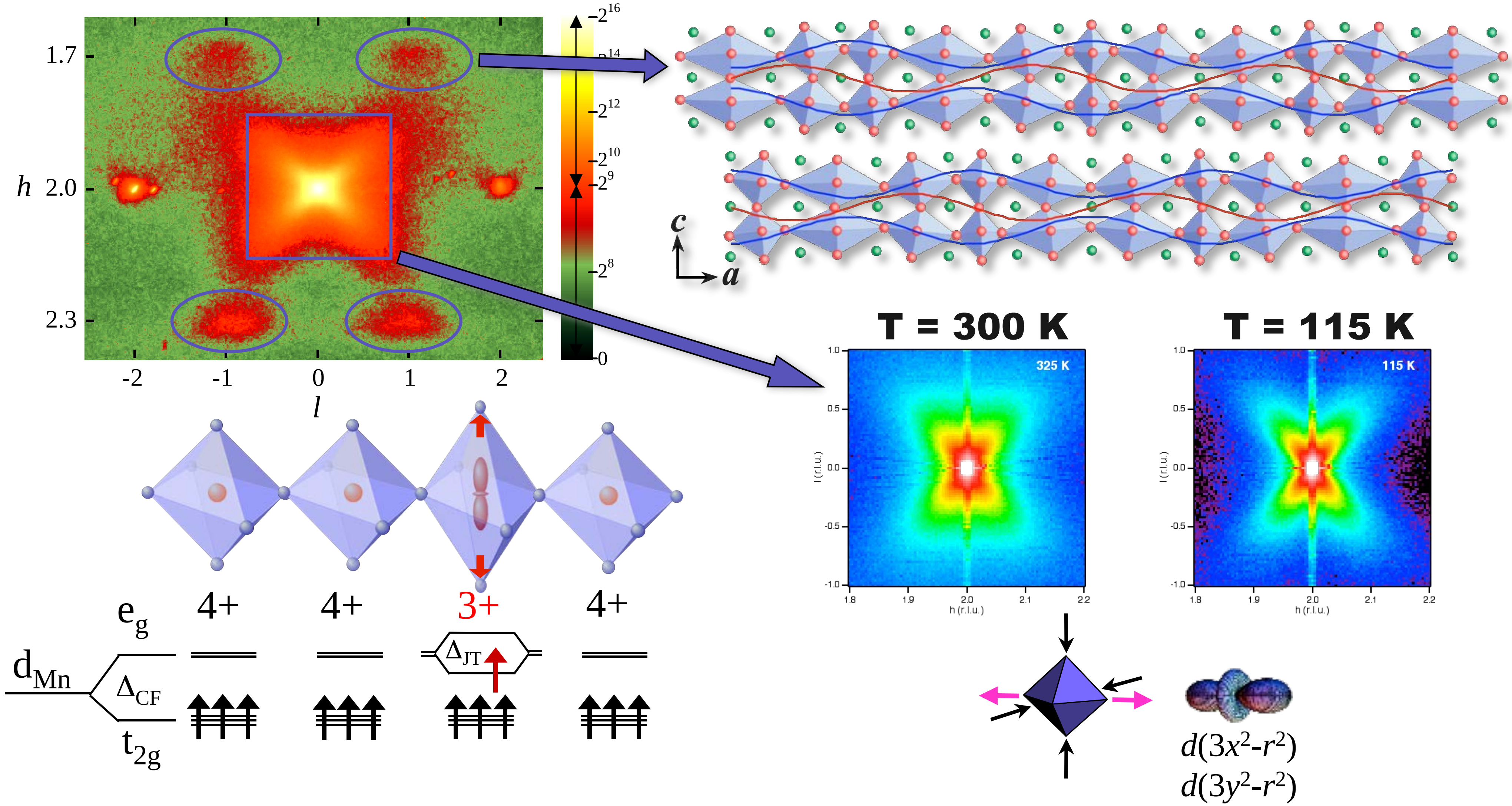

Incommensurate Modulations in $Sr_{0.5}Ba_{0.5}NbO_6$

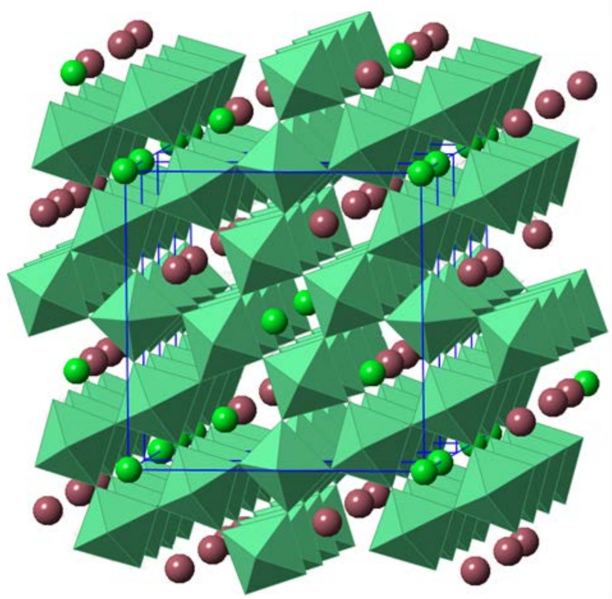

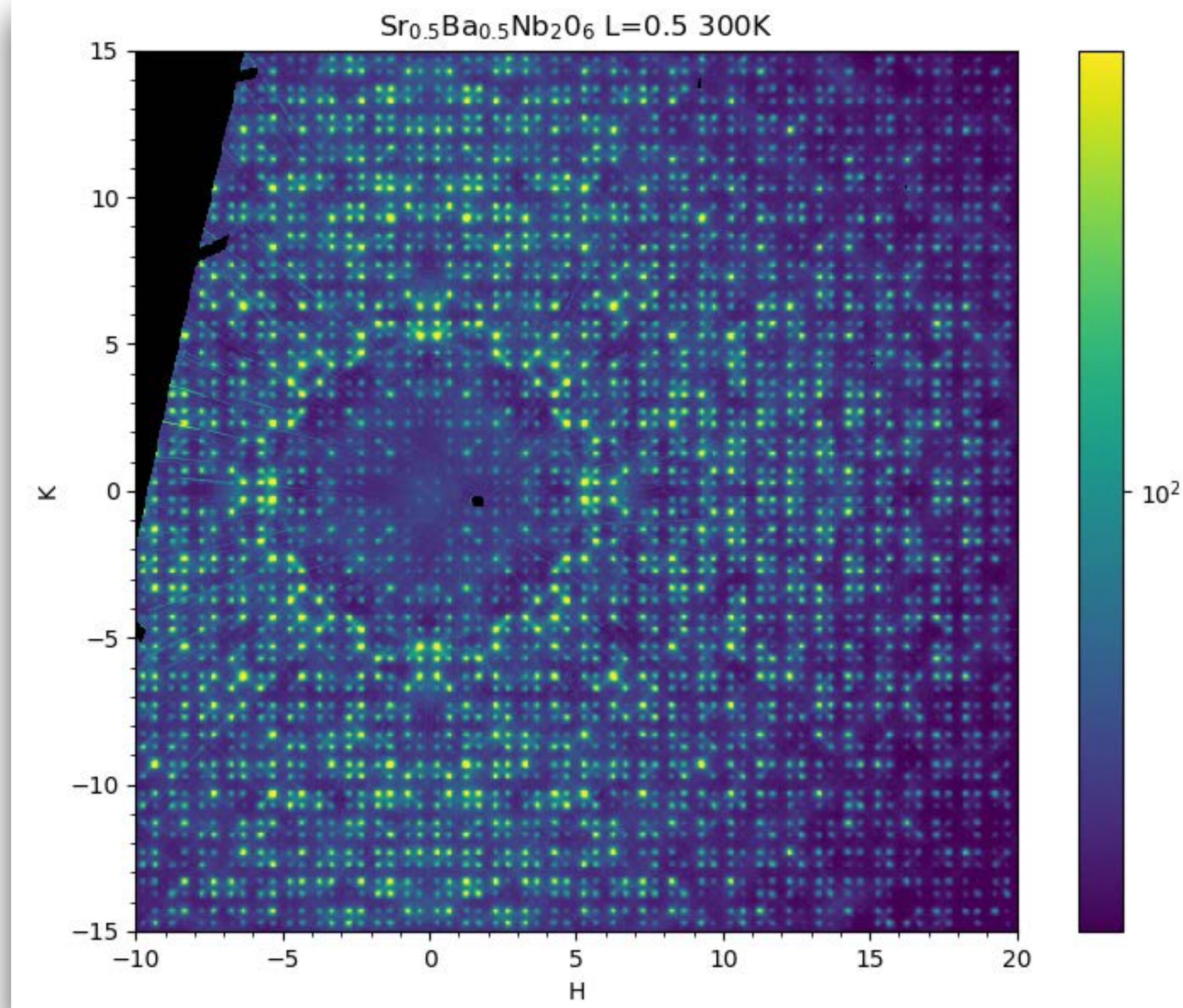

Acknowledgements:
Bixia Wang and Daniel Phelan

Magnetic Diffuse Scattering from Geometric Frustration

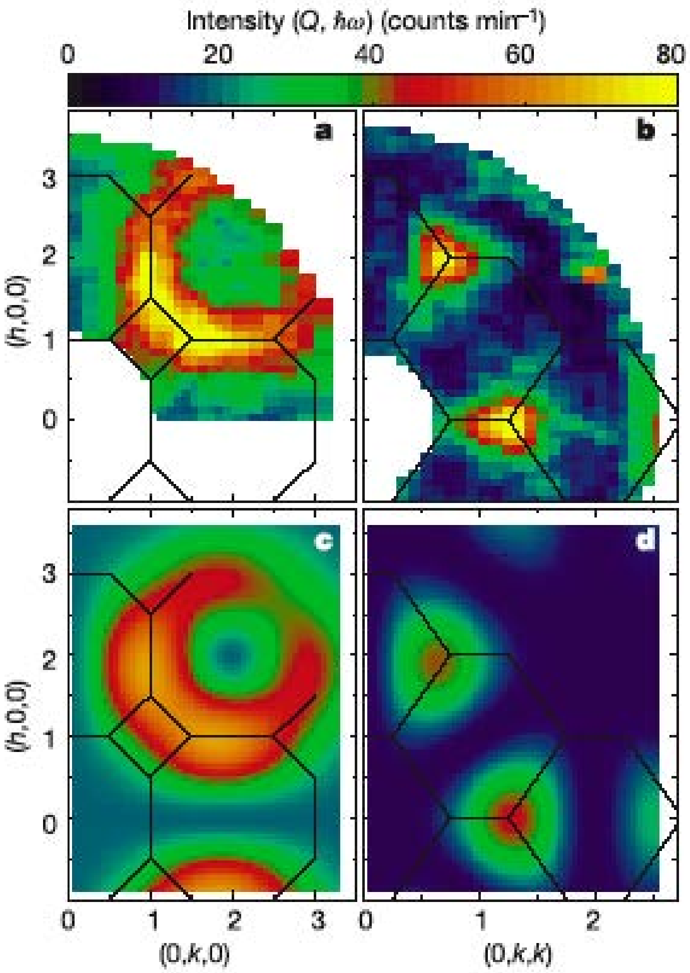

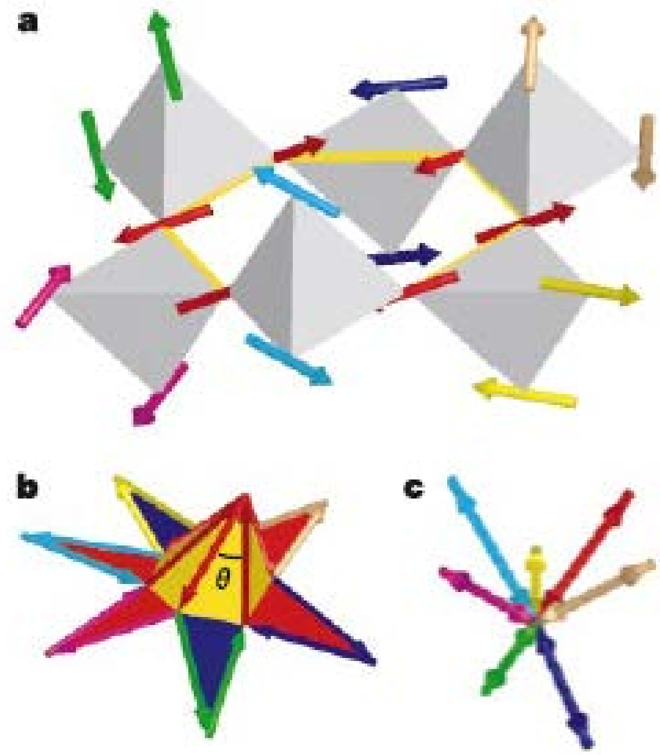

$ZnCr_2O_4$

S.-H. Lee *et al* Nature **418**, 856 (2002)

How do I model it?

A Few Equations

V. M. Nield and D. A. Keen *Diffuse Neutron Scattering From Crystalline Materials* (2001)
T. R. Welberry *Diffuse X-ray Scattering and Models of Disorder* (2004)

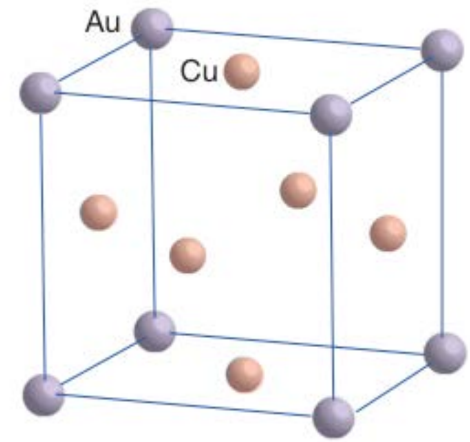

J. M. Cowley, J. Appl. Phys. **21**, 24 (1950)

$$I = \sum_i \sum_j b_i b_j \exp(i\mathbf{Q} \cdot \mathbf{r}_{ij})$$

- **Laue Monotonic Diffuse Scattering**

$$I = \bar{b}^2 \sum_{ij} \exp(i\mathbf{Q} \cdot \mathbf{r}_{ij}) + N(\overline{b^2} - \bar{b}^2);\ \bar{b}^2 = (c_A b_A + c_B b_B)^2;\ \overline{b^2} = c_A c_B (b_B - b_A)^2$$

- **Cowley Short-Range Order**

$$I_{diffuse} = N c_A c_B (b_B - b_A)^2 + \sum_{ij} \alpha_{ij} c_B c_A (b_B - b_A)^2 \exp(i\mathbf{Q} \cdot \mathbf{r}_{ij});\ \alpha_{ij} = \left(1 - \frac{P_{ij}}{c_j}\right)$$

- **Warren Size Effect**

$$I_{diffuse} = N c_A c_B (b_B - b_A)^2 \left(1 + \sum_{ij} \alpha_{ij} \exp(i\mathbf{Q} \cdot \mathbf{r}_{ij}) + \beta_{ij} \exp(i\mathbf{Q} \cdot \mathbf{r}_{ij})\right);\ \beta_{ij} = f(\epsilon_{AA}^{ij}, \epsilon_{BB}^{ij})$$

- **Borie and Sparks Correlations**

$$I = \sum_i \sum_j b_i b_j \exp\left(i\mathbf{Q} \cdot (\mathbf{R}_i - \mathbf{R}_j)\right) \left[1 + i\mathbf{Q} \cdot (\mathbf{u}_i - \mathbf{u}_j) - \frac{1}{2} \left(\mathbf{Q} \cdot (\mathbf{u}_i - \mathbf{u}_j)\right)^2 + \ldots\right]$$

Thermal Diffuse Scattering

- Lattice vibrations produce deviations from the average structure even in perfect crystals
- X-ray scattering intensity is given by the integral over all the phonon branches at each **Q**

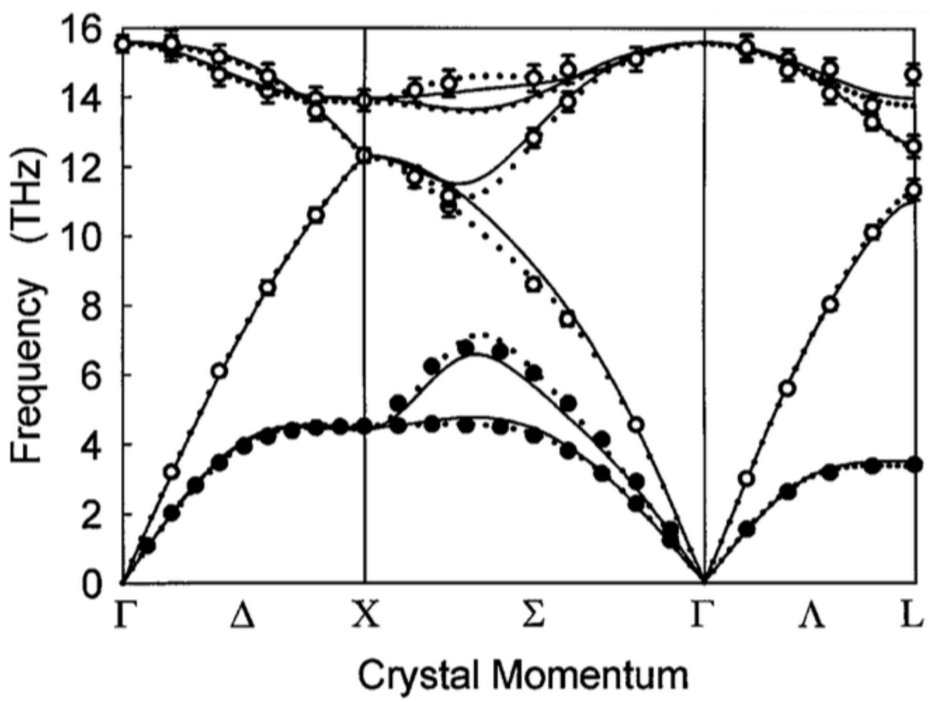

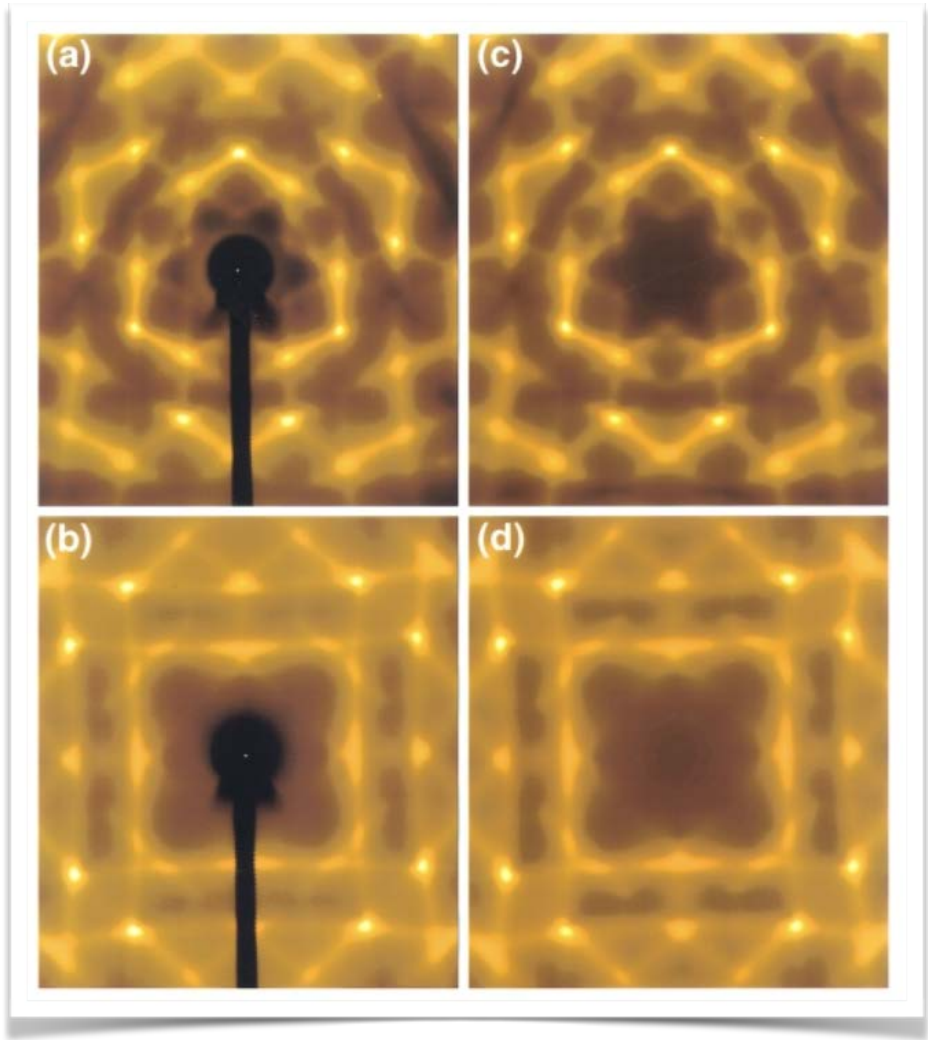

$$I_0 \propto f^2 e^{-2M} \sum_{j=1}^{6} \frac{|\mathbf{q} \cdot \hat{\mathbf{e}}_j|^2}{\omega_j} \coth\left(\frac{\hbar\omega_j}{2k_B T}\right).$$

M. Holt, *et al*, Phys Rev Lett **83**, 3317 (1999).

Some Rules of Thumb (*thanks to* Hans Beat Bürgi)

Reciprocal space		Direct space
Only sharp Bragg reflections	→	3D-periodic structure - no defects
Sharp diffuse rods	→	2D-periodic structure - perpendicular to the streaks - disordered in streak directions
Sharp diffuse planes	→	1D-periodic structure - perpendicular to the planes - disordered within the plane
Diffuse clouds	→	0D-periodic structure - no fully ordered direction

Case Study 1: Mullite

Mullite - A Case Study

- Mullite is a ceramic that is formed by adding O^{2+} vacancies to Sillimanite
  - Sillimanite has alternating AlO_4 and SiO_4 tetrahedra
  - Mullite has excess Al^{3+} occupying Si^{2+} sites for charge balance
- This results in strong vacancy-vacancy correlations

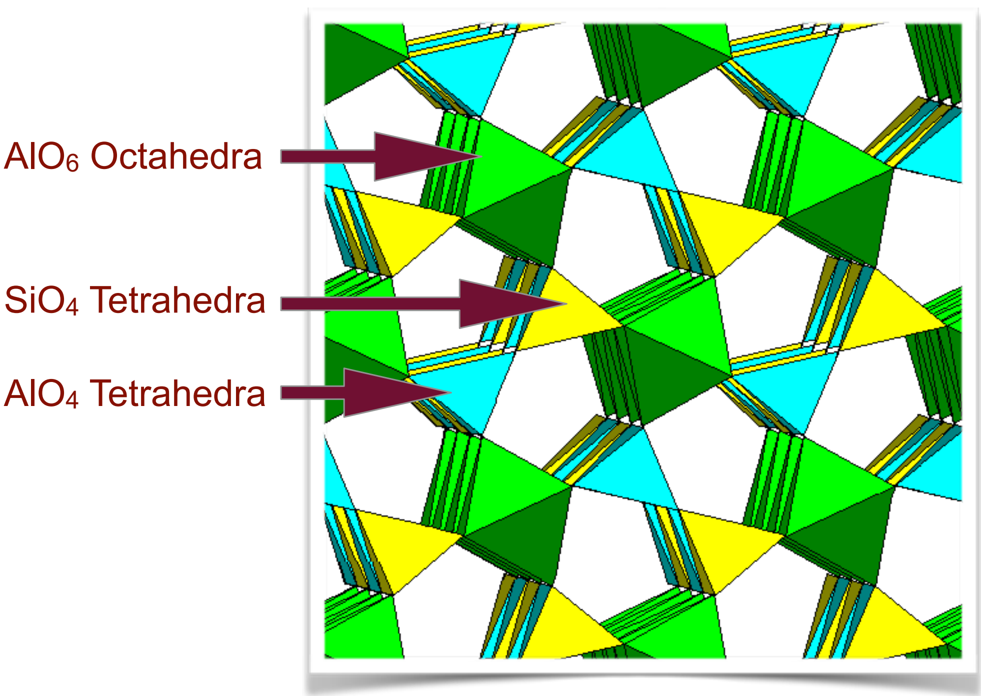

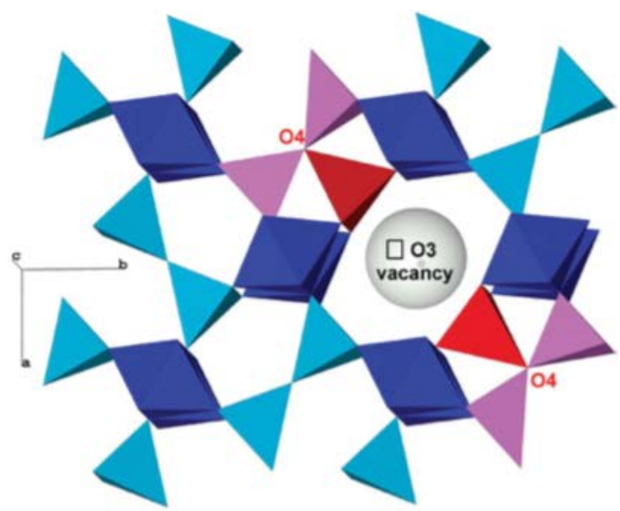

Sillimanite: Al_2SiO_5

Mullite: $Al_2(Al_{2+2x}Si_{2-2x})O_{10-x}$

B. D. Butler, T. R. Welberry, & R. L. Withers, Phys Chem Minerals **20**, 323 (1993)

Measuring X-ray Diffuse Scattering with Continuous Rotation Method

Incident Beam

Detector

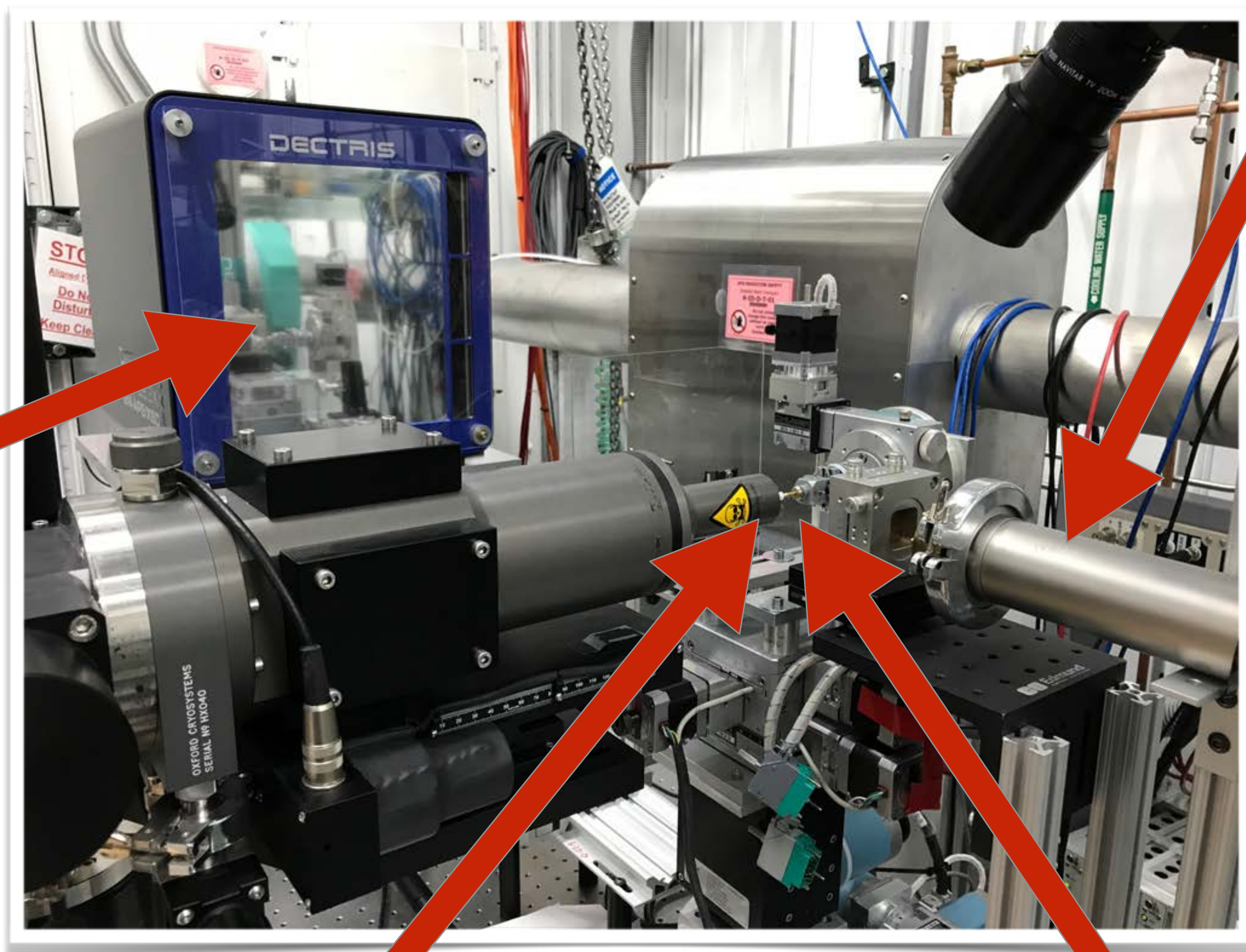

Cryocooler

Sample

Measuring X-ray Diffuse Scattering with Continuous Rotation Method

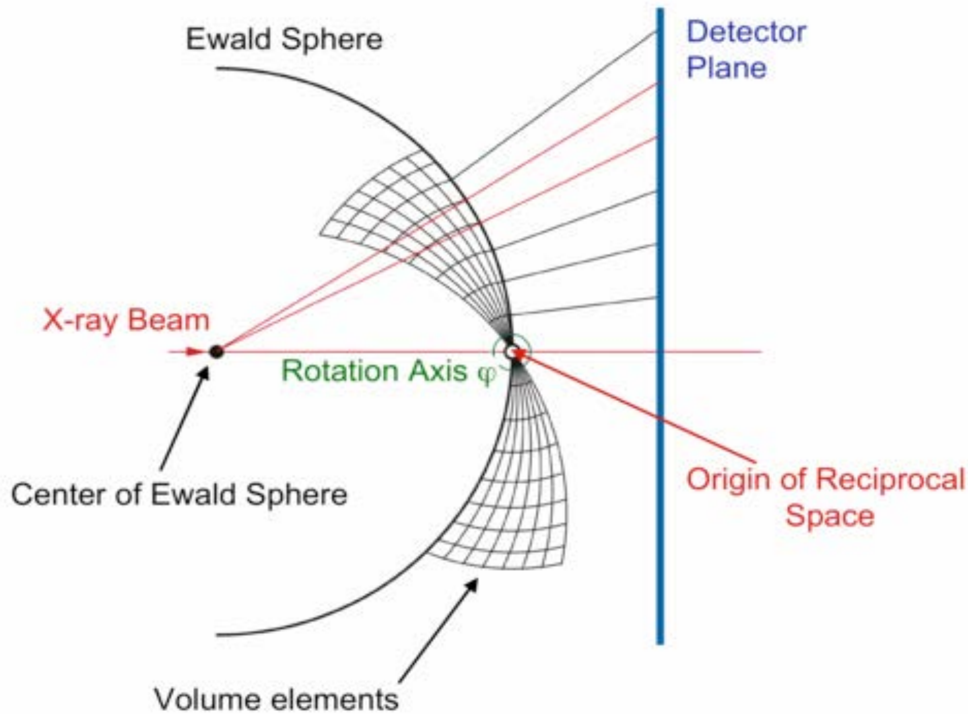

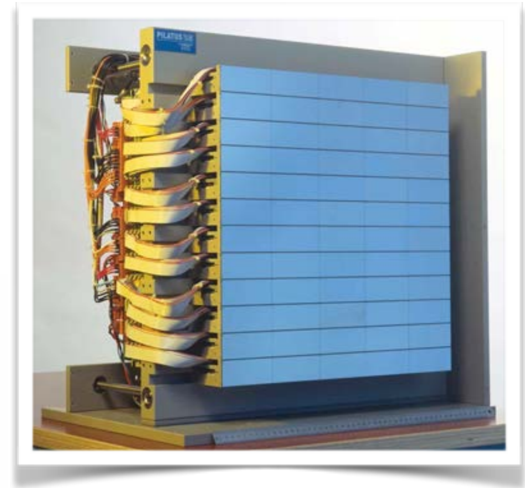

Pilatus 2M Detector

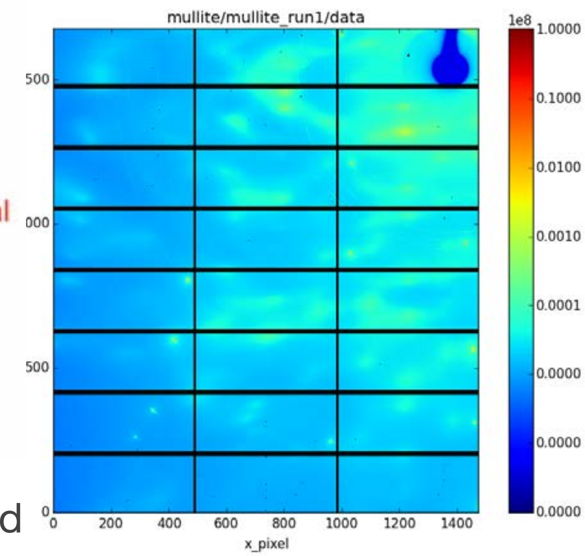

- The sample is continuously rotated in shutterless mode at 1° per second
- A fast area detector (*e.g.*, a Pilatus 2M) acquires images at 10 frames per second
  - *i.e.,* 3600 x 8MB frames ~ 30GB every 6 minutes
- The detector needs low background, high dynamic range, and energy discrimination
  - Ideally, this is performed with high-energy x-rays, *e.g.*, 80 to 100 keV

Experiment Workflow

- Powder calibration to determine detector distance, centers, and tilts
- Bragg peak search to optimize the sample/detector geometry
- Determine the orientation matrix
- Perform coordinate transformation at each detector position
- Merge the three transforms

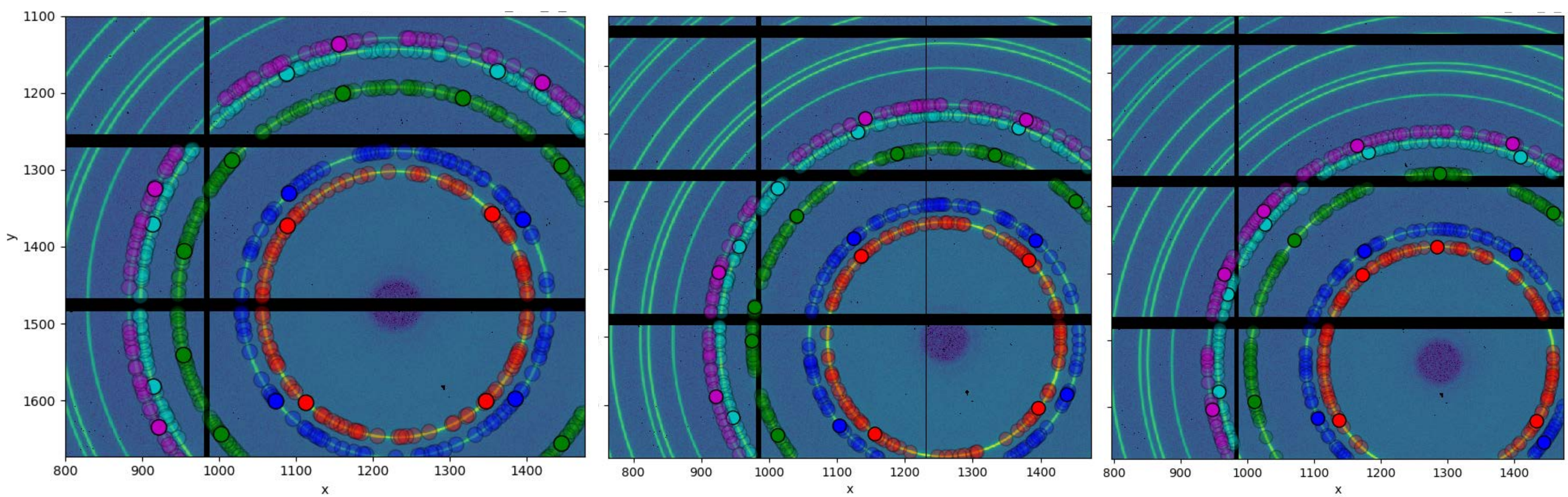

Diffuse Scattering in the Relaxor $PbMg_{1/3}Nb_{2/3}O_3$

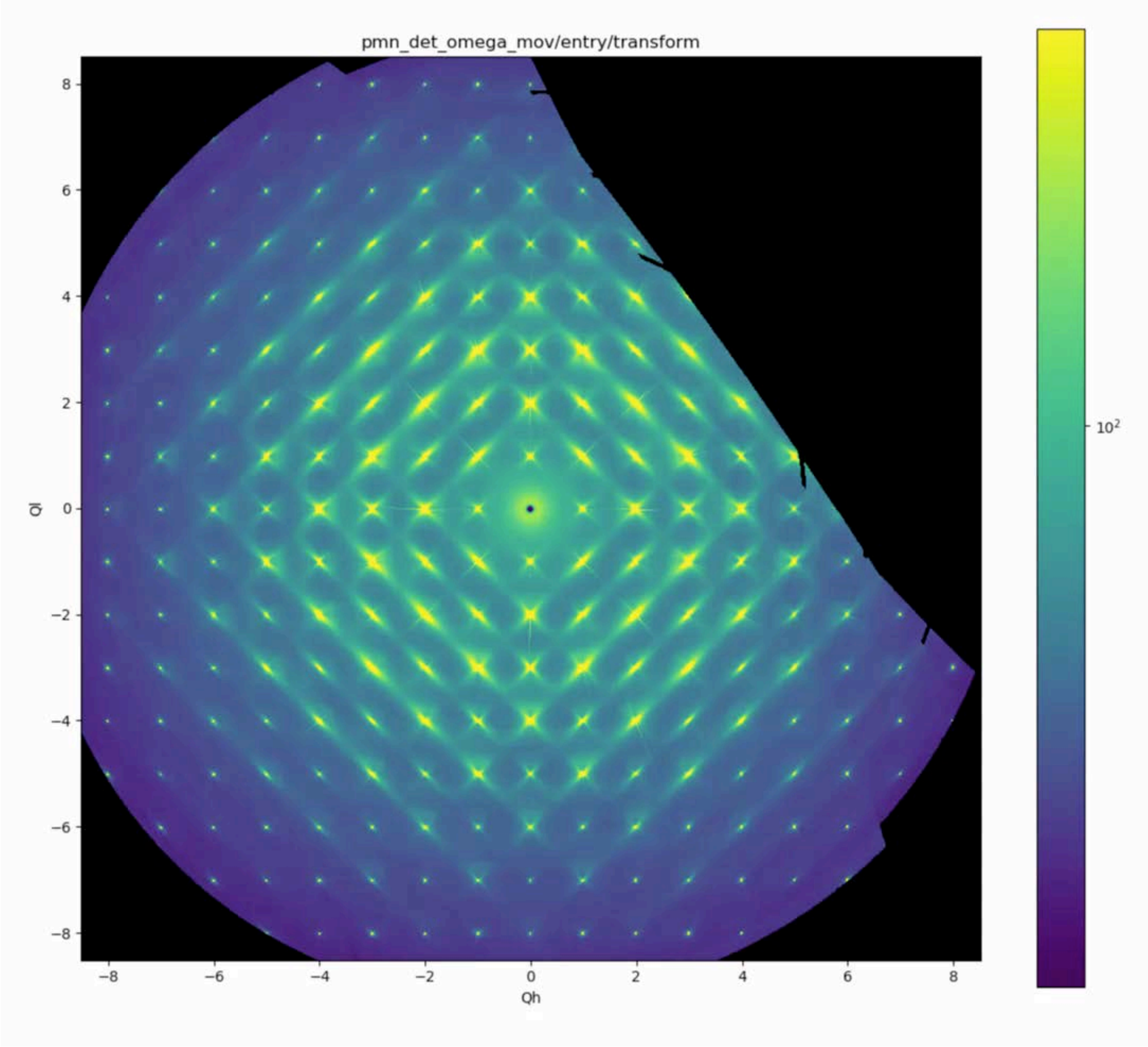

3D Diffuse Scattering in Mullite

- There is strong diffuse scattering throughout reciprocal space
- The shape of the diffuse scattering is strongly dependent on the value of QI
- There are incipient superlattice peaks at **Q** = 0.5 c^* + 0.31 a^*

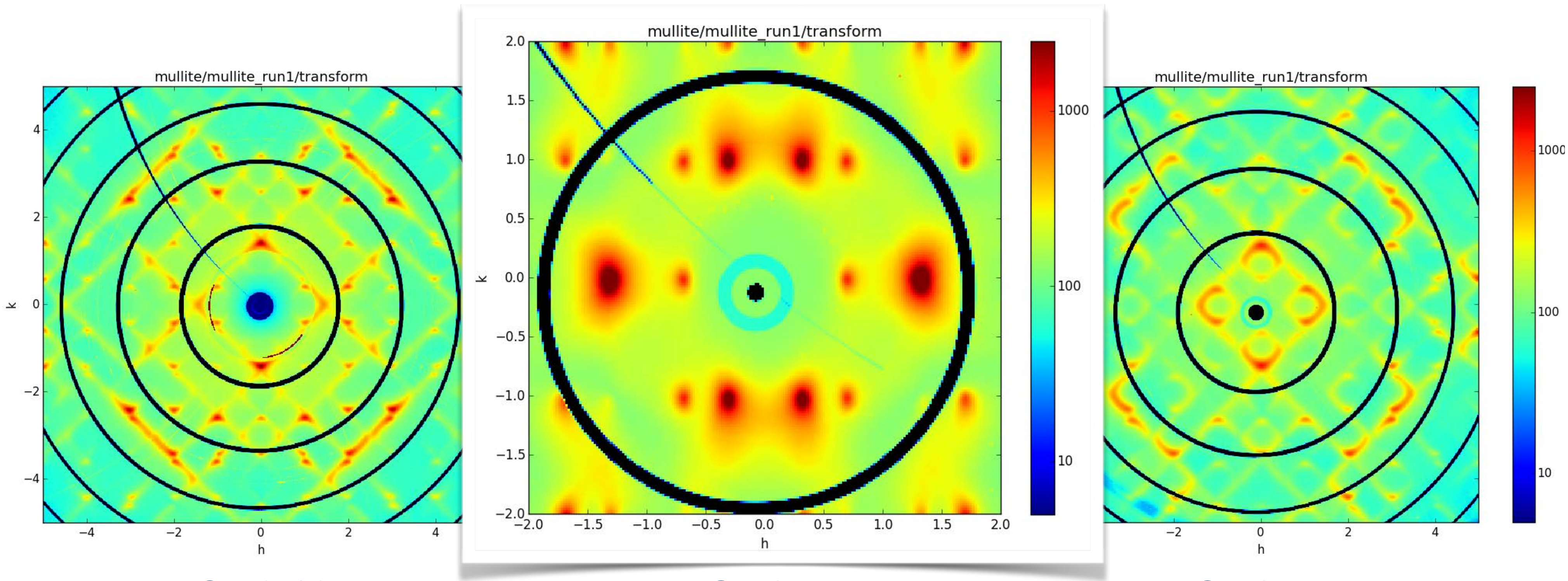

QI=0.16 QI=0.5 QI=0.75

Monte Carlo Analysis

- In a classic analysis, Richard Welberry and colleagues developed a set of interaction energies to model mullite disorder
- Interaction energies were initialized:
  - insights from chemical intuition
  - insights from the measured diffuse scattering
- The diffuse scattering was calculated using a Monte Carlo algorithm to generate vacancy distributions first in 2D slices and then in 3D

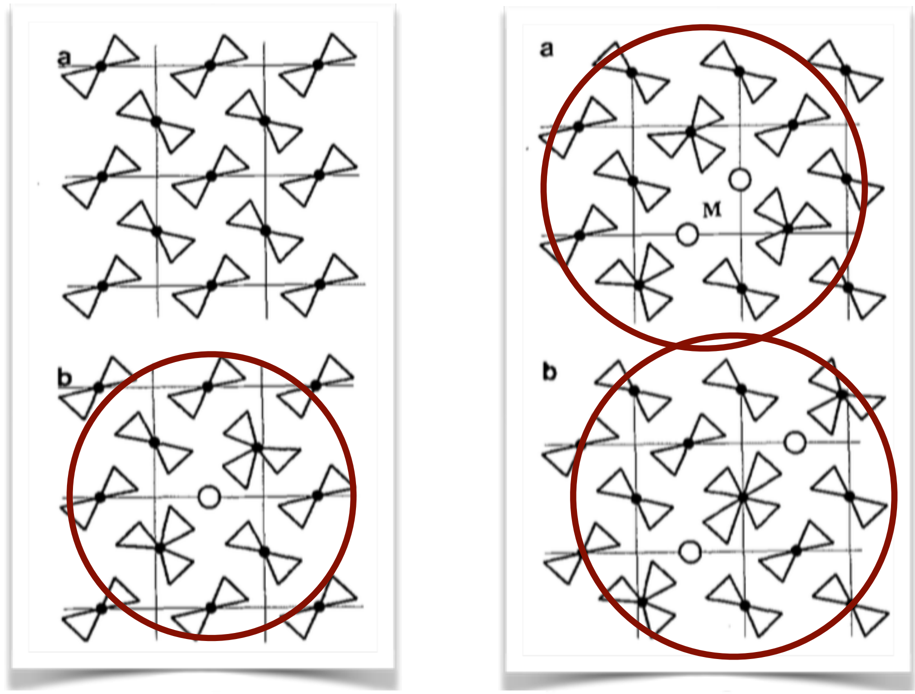

$$P_i = \frac{e^{-V_i}}{1+e^{-V_i}},$$

where,

$$V_i = \frac{\sum_j E_{ij}}{kT} + \frac{(N_v - N_v^o)^2}{N_v^o} \operatorname{sgn}(N_v - N_v^o).$$

Interatomic vector	α_{lmn}	Interatomic vector	α_{lmn}
$\frac{1}{2}\langle 1\ 1\ 0 \rangle$	−0.24	$\langle 0\ 2\ 0 \rangle$	+0.13
[1 1 0]	−0.23	$\frac{1}{2}\langle 3\ 1\ 0 \rangle$	+0.22
[1 −1 0]	−0.05	$\frac{1}{2}\langle 1\ 3\ 0 \rangle$	−0.01
$\langle 1\ 0\ 0 \rangle$	−0.06	$\langle 1\ 0\ 1 \rangle$	+0.07
$\langle 0\ 1\ 0 \rangle$	+0.22	$\langle 0\ 1\ 1 \rangle$	−0.12
$\langle 0\ 0\ 1 \rangle$	−0.03	$\frac{1}{2}\langle 3\ 3\ 0 \rangle$	+0.17
$\frac{1}{2}$[1 −1 2]	+0.12	$\langle 1\ 1\ 1 \rangle$	−0.01
$\frac{1}{2}$[1 1 2]	+0.12	$\frac{1}{2}\langle 3\ 1\ 2 \rangle$	−0.11
$\langle 2\ 0\ 0 \rangle$	−0.12	$\frac{1}{2}\langle 3\ 3\ 2 \rangle$	−0.07

B. D. Butler, T. R. Welberry, & R. L. Withers, Phys Chem Minerals **20**, 323 (1993)

Monte Carlo Analysis Results

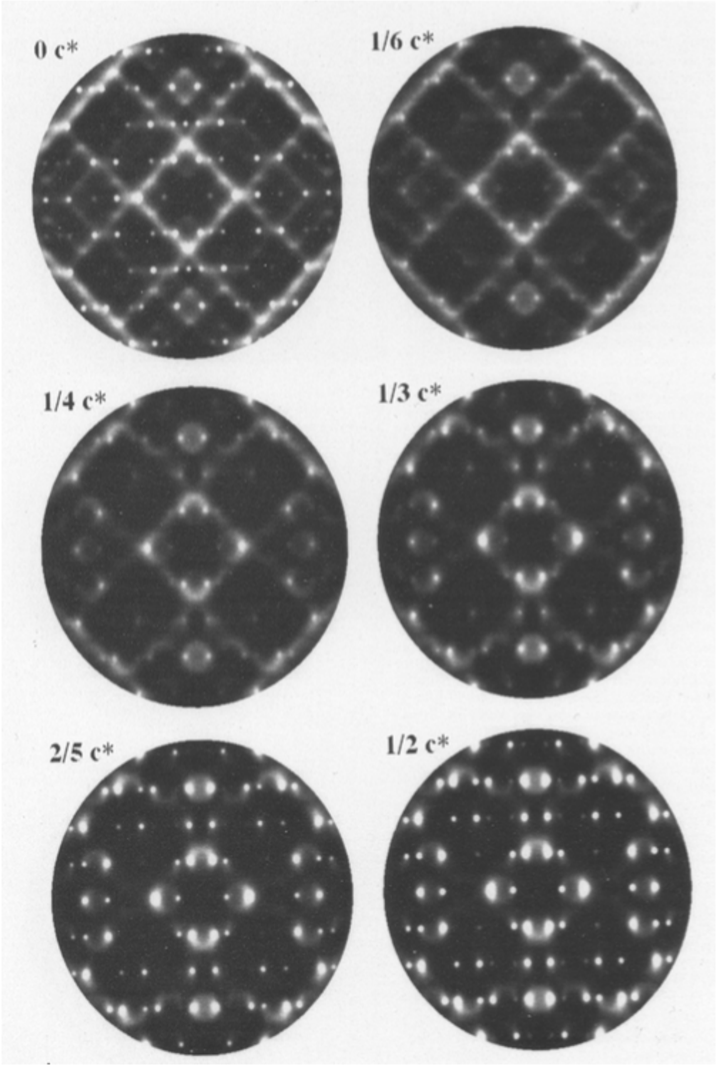

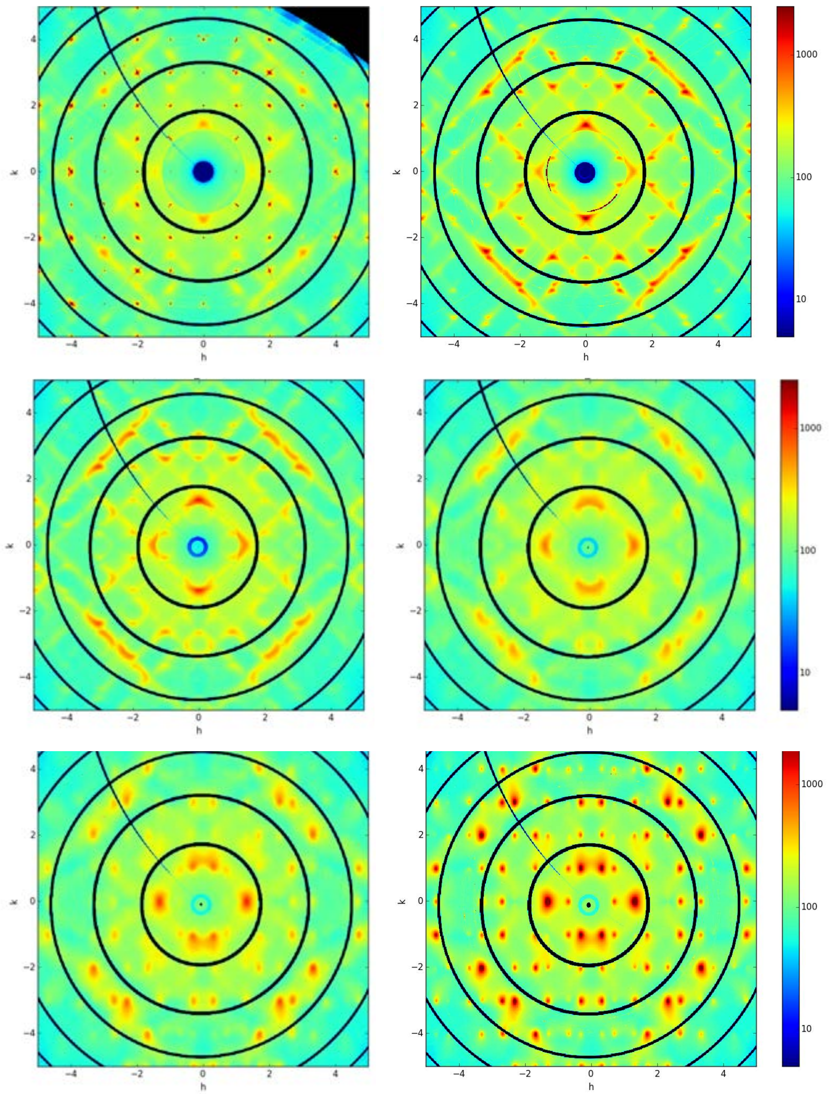

Vacancy Short-Range Order in Mullite

A First-Principles Approach (*ab initio* HRMC)

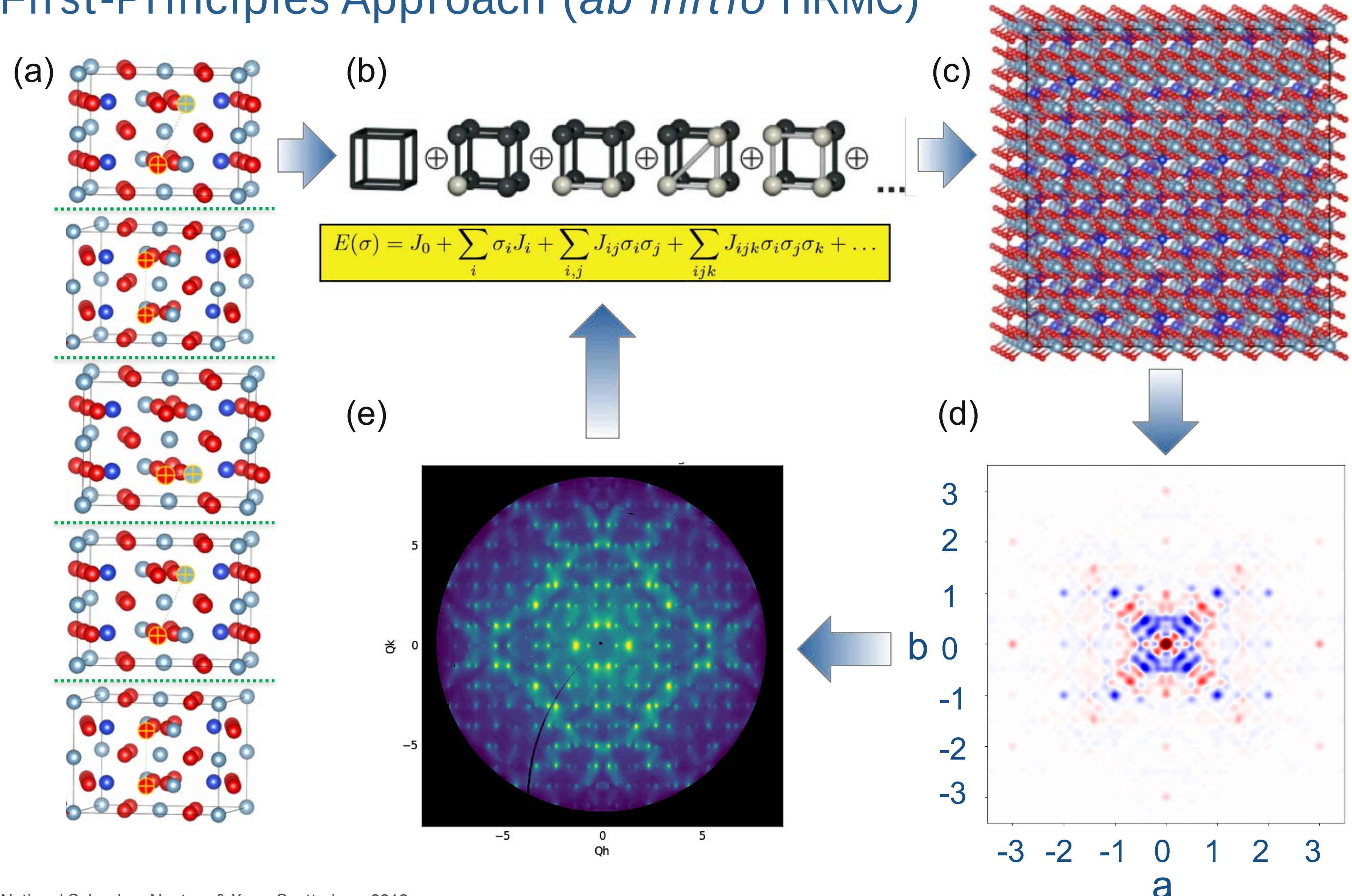

Nearly-Commensurate Vacancy Stripes in Mullite

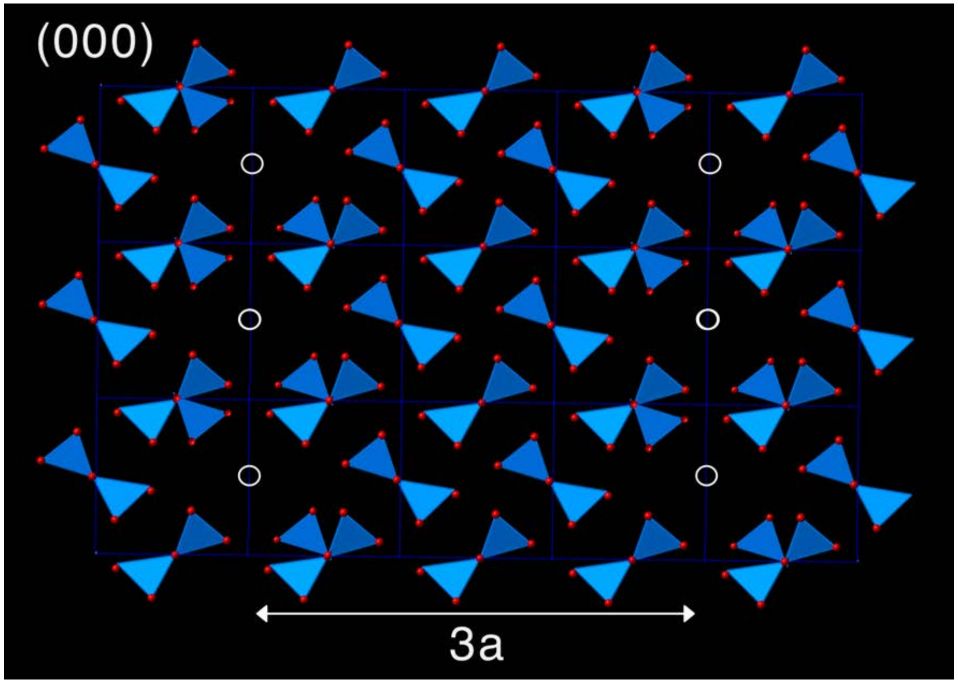

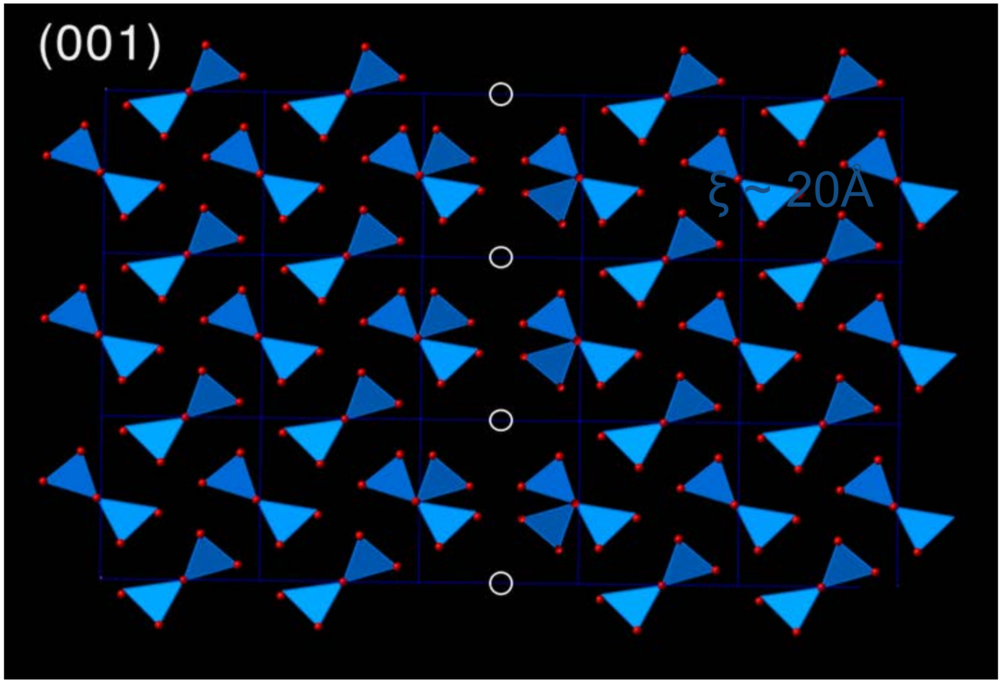

c = 0

c = 1.0

$$\mathbf{q} = \pm\frac{1}{2}\mathbf{c}^* \pm \frac{1}{3}\mathbf{a}^*$$

Case Study 2: Sodium-Intercalated V_2O_5

3D-ΔPDF

Pair Distribution Function Analysis

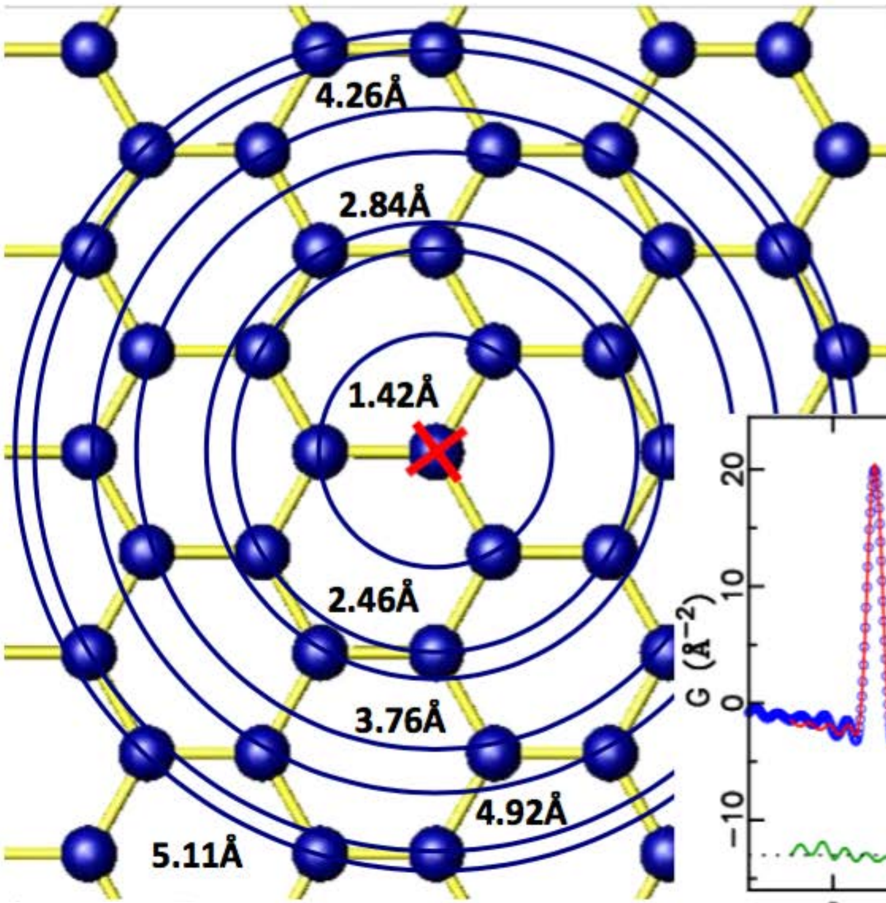

Radial atomic **pair d**istribution **f**unction (PDF) gives the interatomic distance distribution, or "probability" of finding atomic pairs distance *r* apart

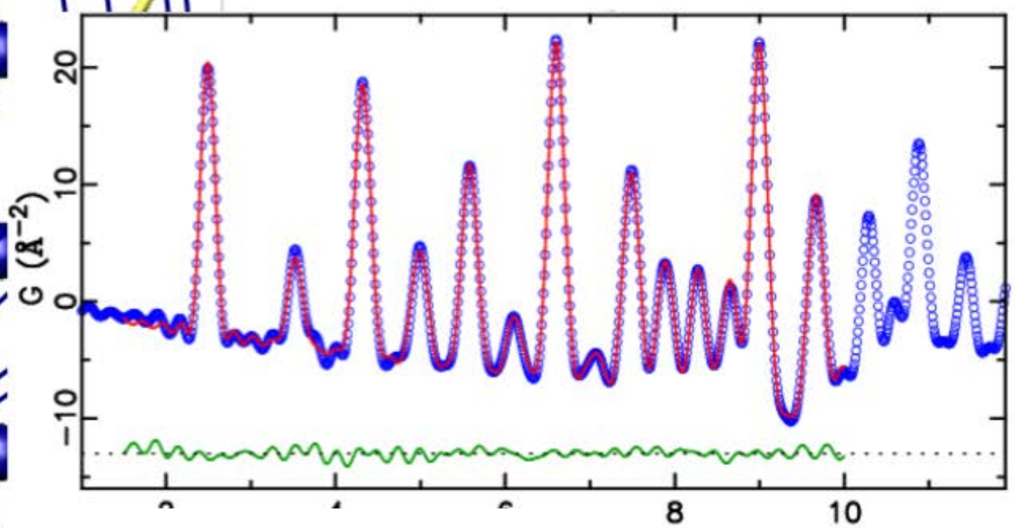

$$G(r) = 4\pi r[\rho(r) - \rho_o] = (2/\pi) \int_{Q=Q_{min}}^{Q_{max}} Q[S(Q)-1]\sin(Qr)\,dQ$$

Emil Bozin (ADD 2013)

Three-Dimensional Pair Distribution Functions

- The ability to measure three-dimensional S(**Q**) over a wide range of reciprocal space provides the 3D analog of PDF measurements.
  - Total PDFs if Bragg peaks and diffuse scattering can be measured simultaneously
  - Δ-PDFs if the Bragg peaks are eliminated
    - using the punch and fill method
- This would allow a model-independent view of the measurements in real space.

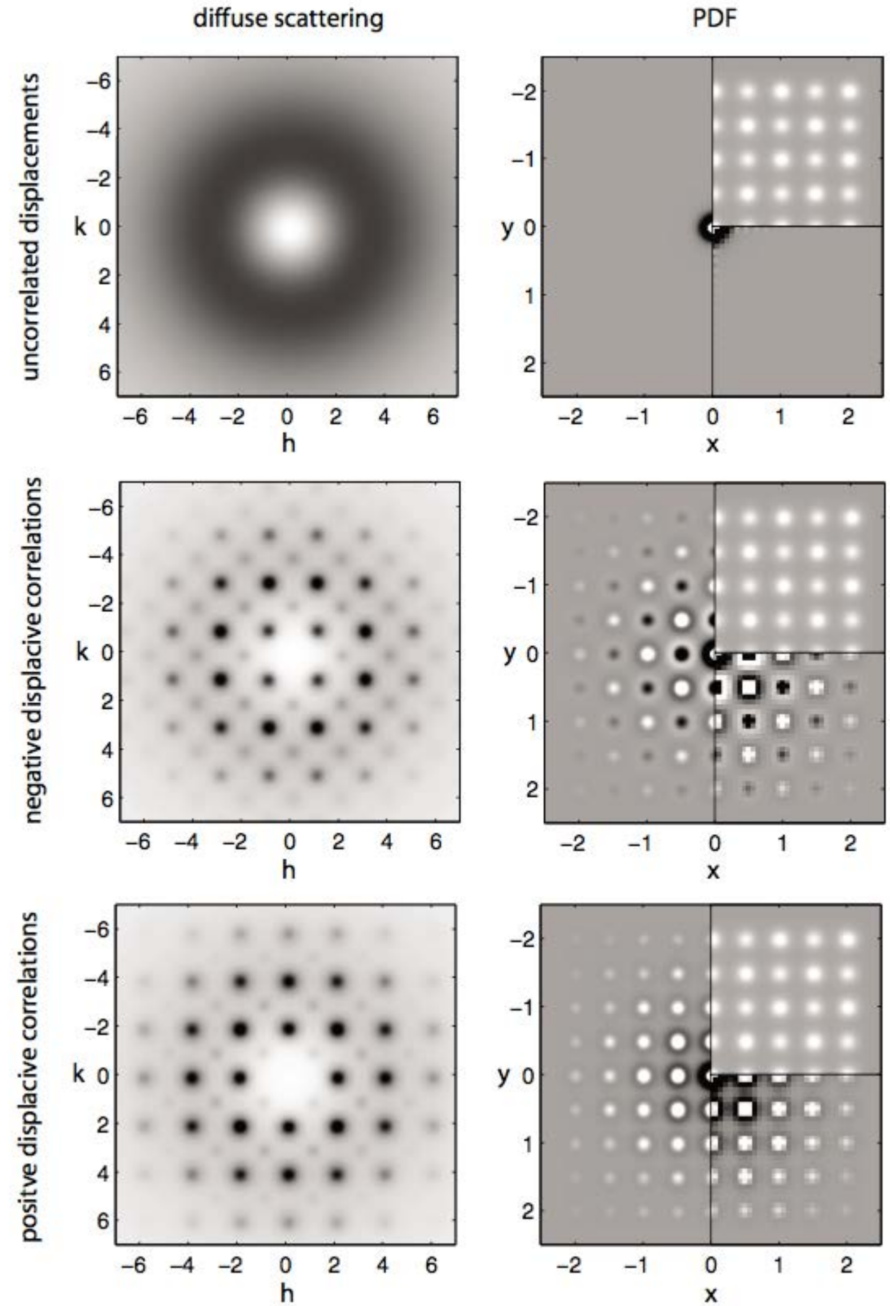

238 Z. Kristallogr. **2012**, *227*, 238–247 / **DOI** 10.1524/zkri.2012.1504

The three-dimensional pair distribution function analysis of disordered single crystals: basic concepts

Thomas Weber* and Arkadiy Simonov

Laboratory of Crystallography, ETH Zurich Wolfgang-Pauli-Str. 10, 8093 Zurich, Switzerland

“Punch and Fill”

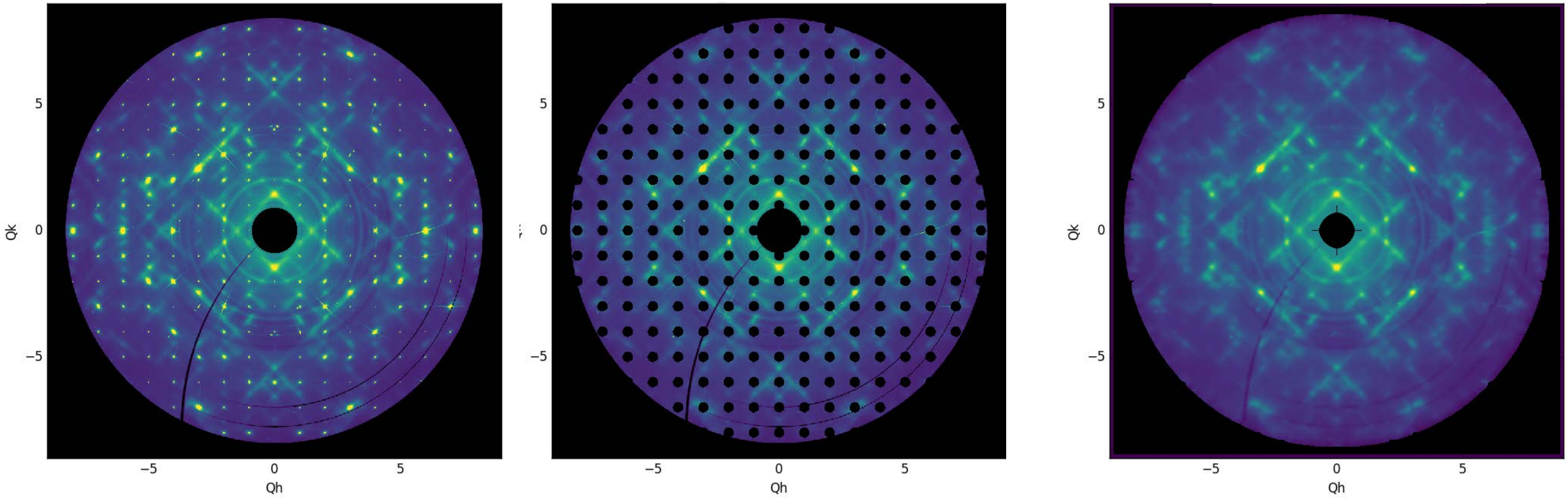

Symmetrize Punch Fill

$$P_{\text{tot}}(\boldsymbol{r}) = FT[I(\boldsymbol{u})] = FT\left[|\bar{F}(\boldsymbol{u})|^2\right] + FT\left[|\Delta F(\boldsymbol{u})|^2\right] = P_{hkl}(\boldsymbol{r}) + \Delta P(\boldsymbol{r})$$

Sodium-Intercalated V_2O_5

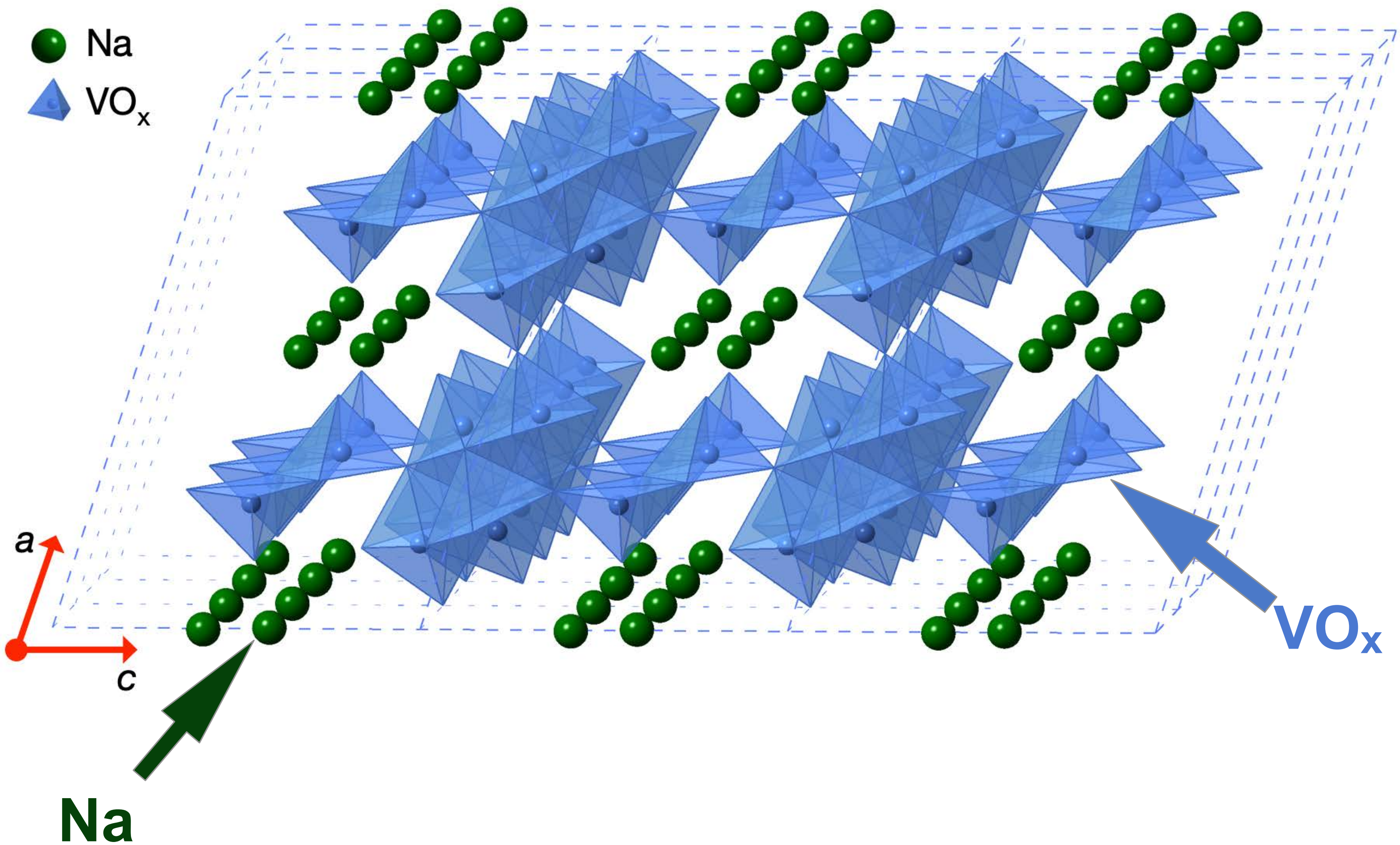

M. J. Krogstad, S. Rosenkranz, J. M. Wozniak, G. Jennings, J. P. C. Ruff, J. T. Vaughey, and R. Osborn
arXiv 1902.03318 (submitted to Nature Materials).

Diffuse Scattering in $Na_{0.2}V_2O_5$ and $Na_{0.4}V_2O_5$

Qk=0.5

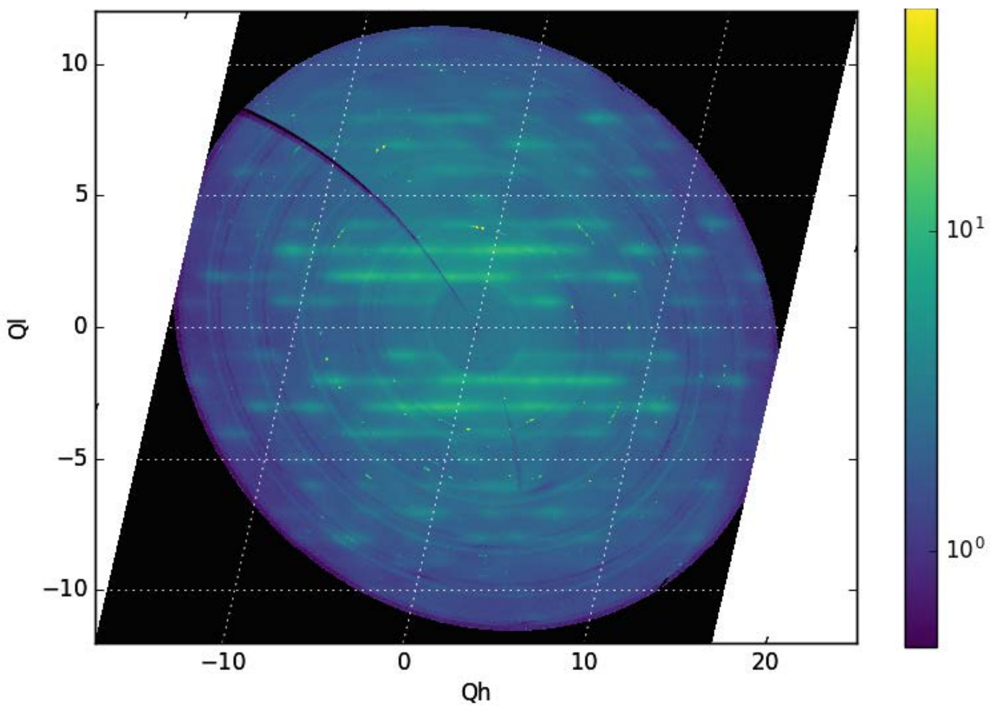

$Na_{0.4}V_2O_5$

300K

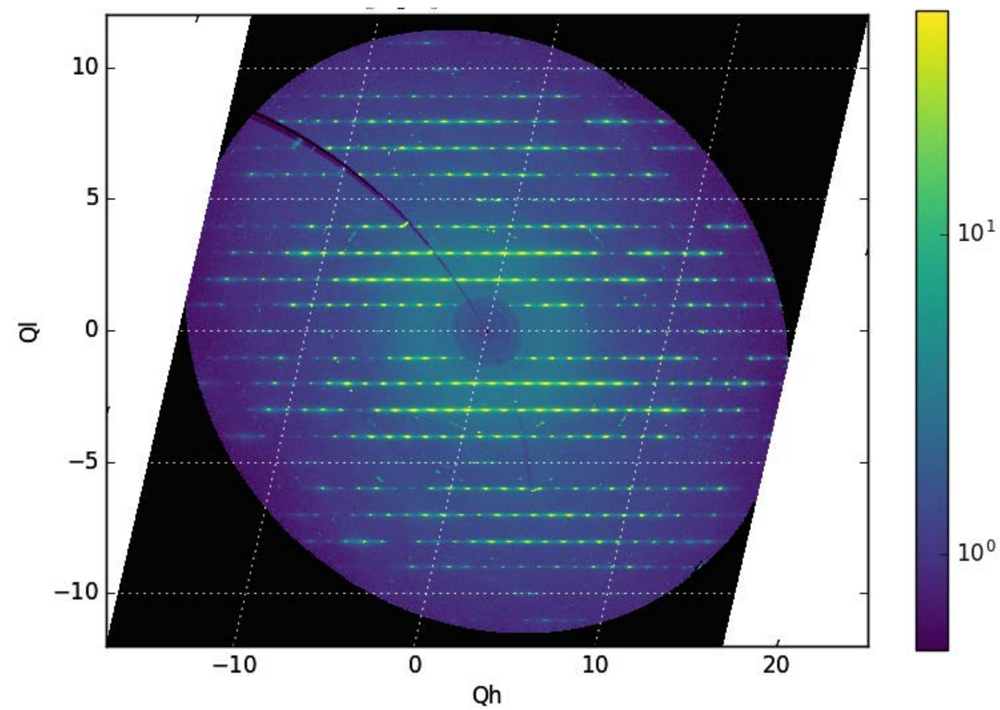

$Na_{0.4}V_2O_5$

100K

Sublattice Melting

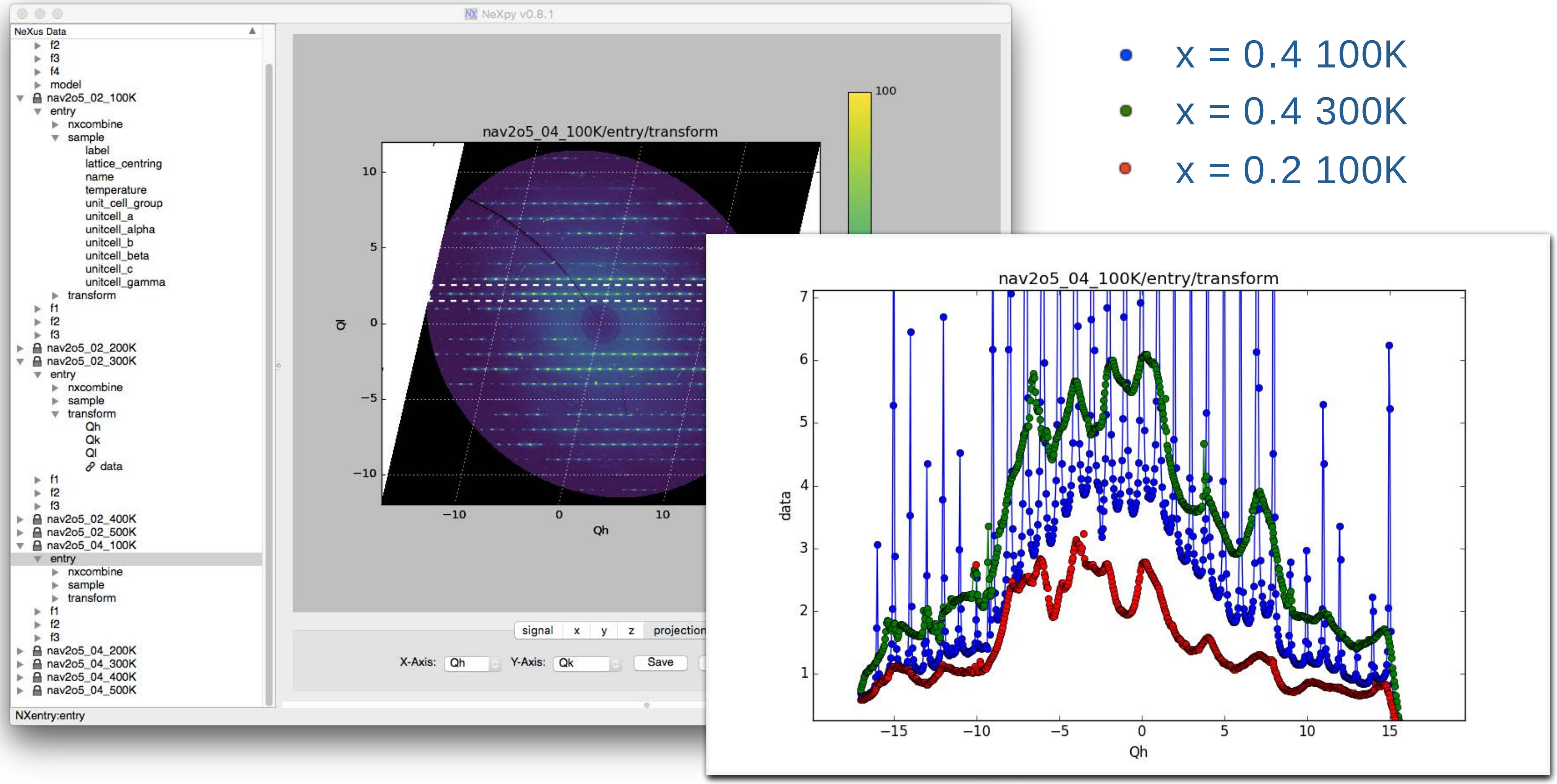

- x = 0.4 100K
- x = 0.4 300K
- x = 0.2 100K

3D-ΔPDF Analysis of

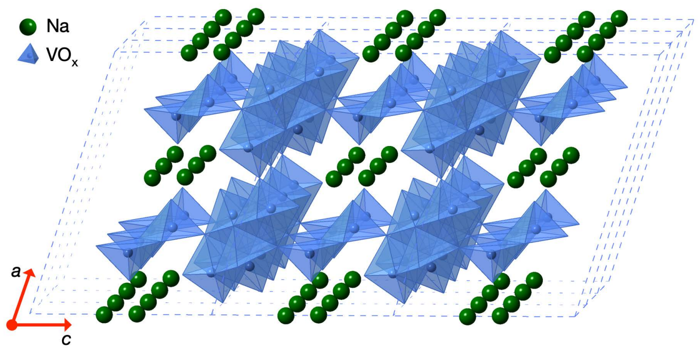

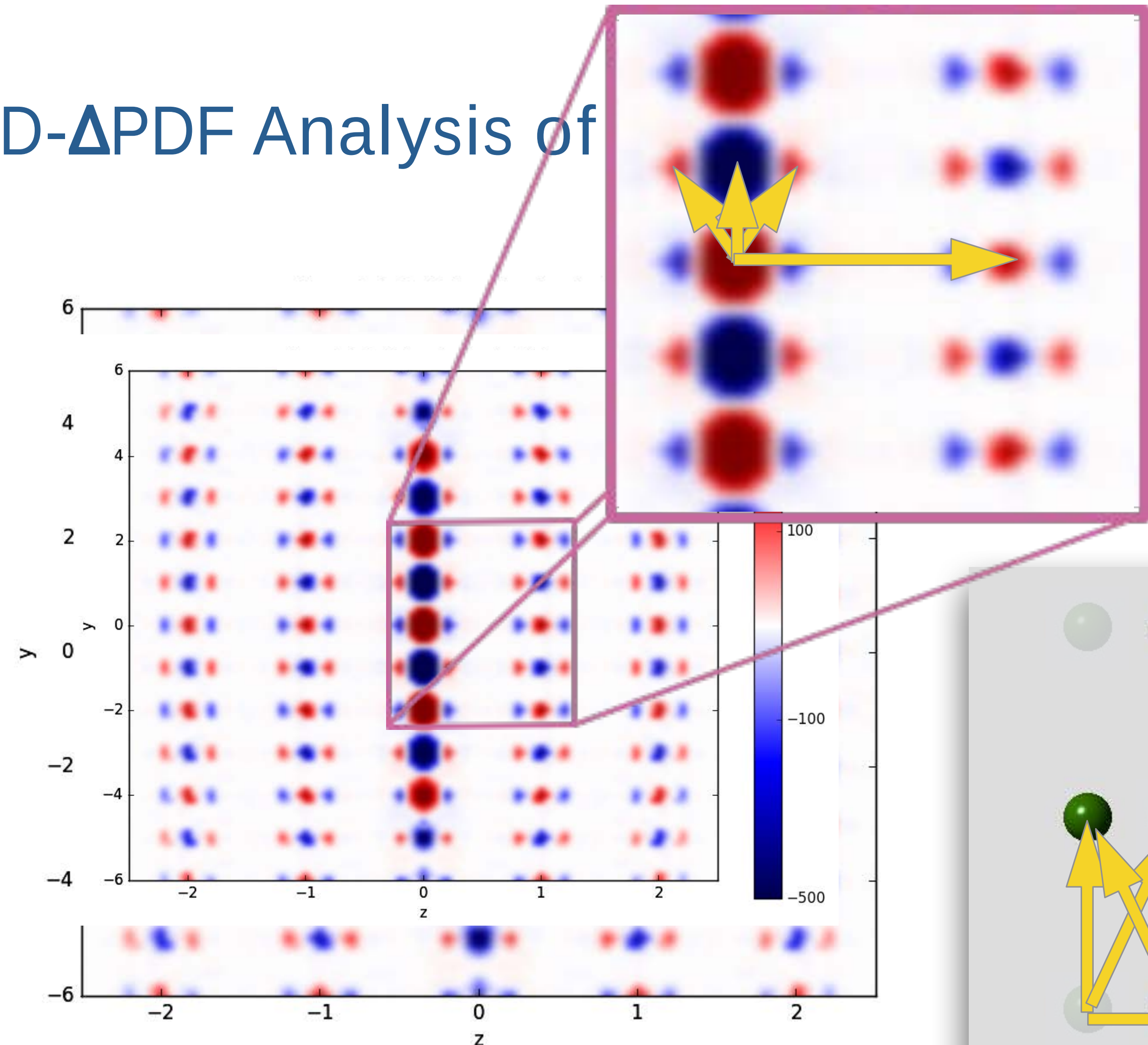

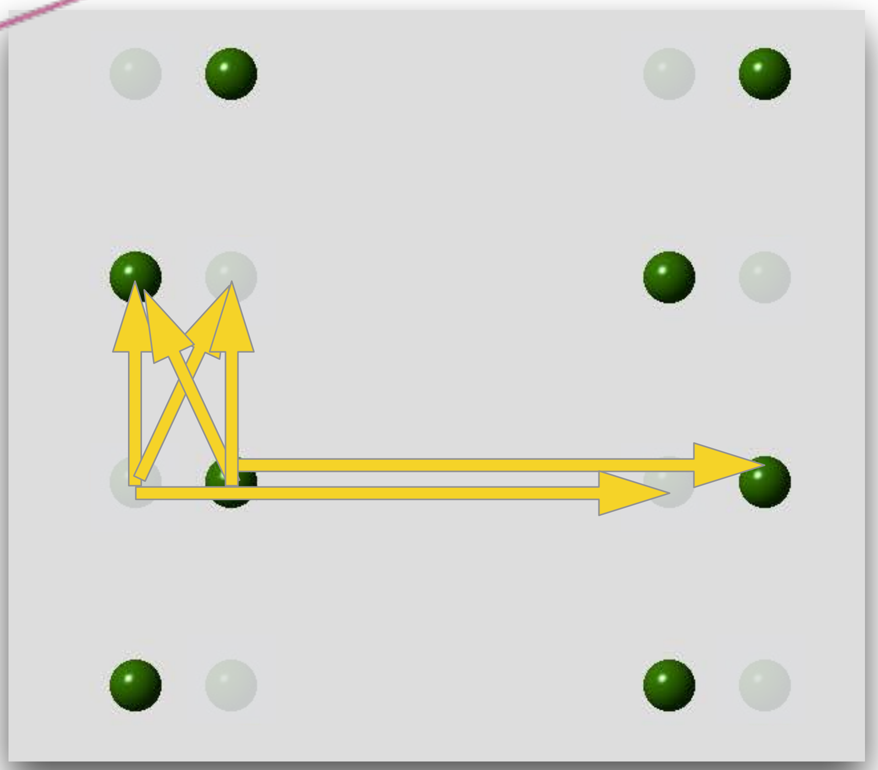

Real Space *vs* 3D-ΔPDF

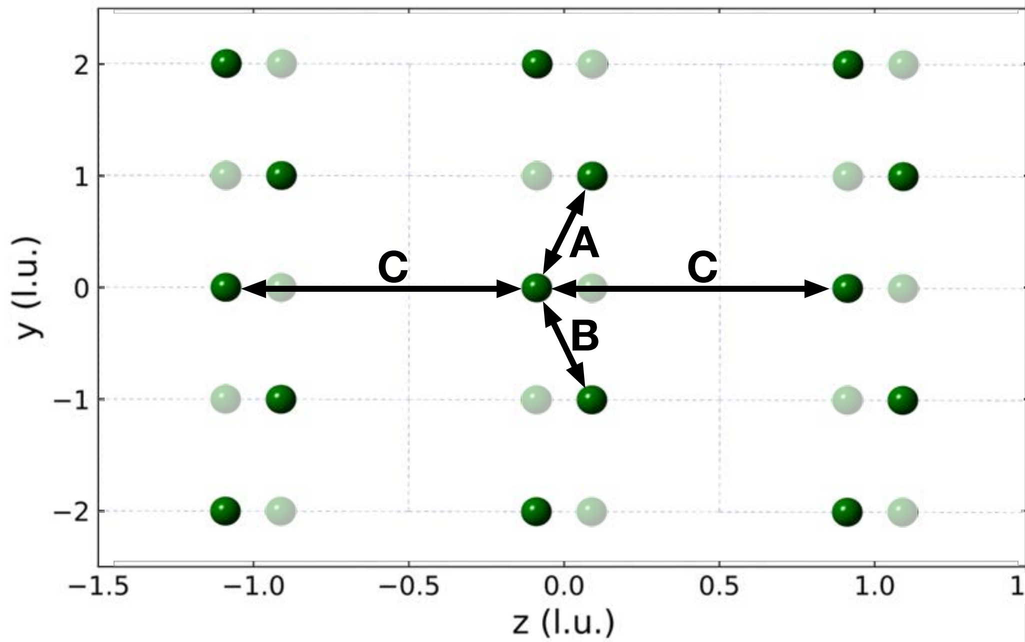

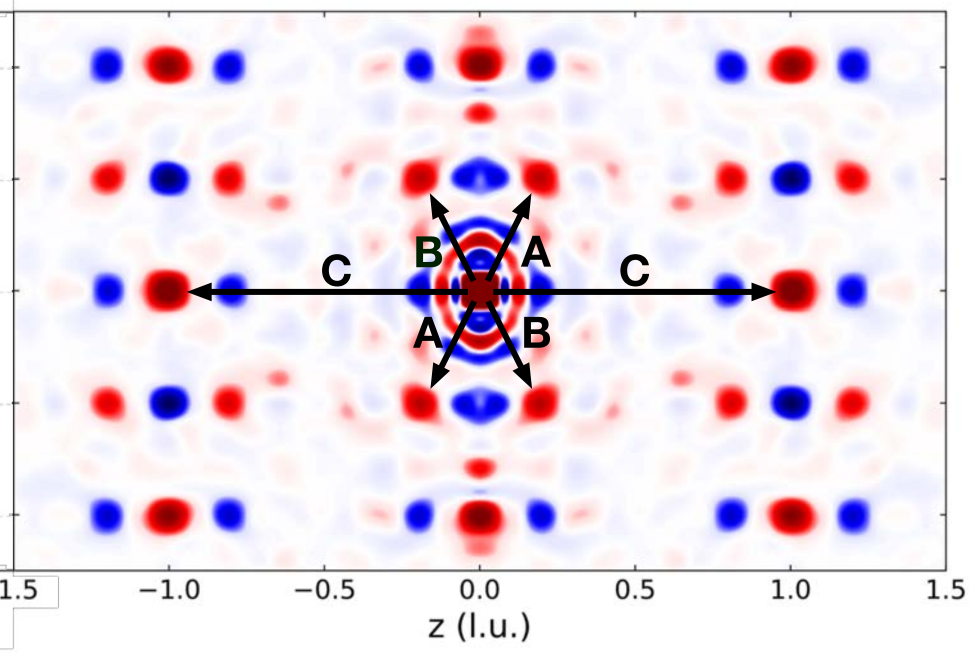

Order-Disorder Transition
Viewed in Reciprocal and Real Space

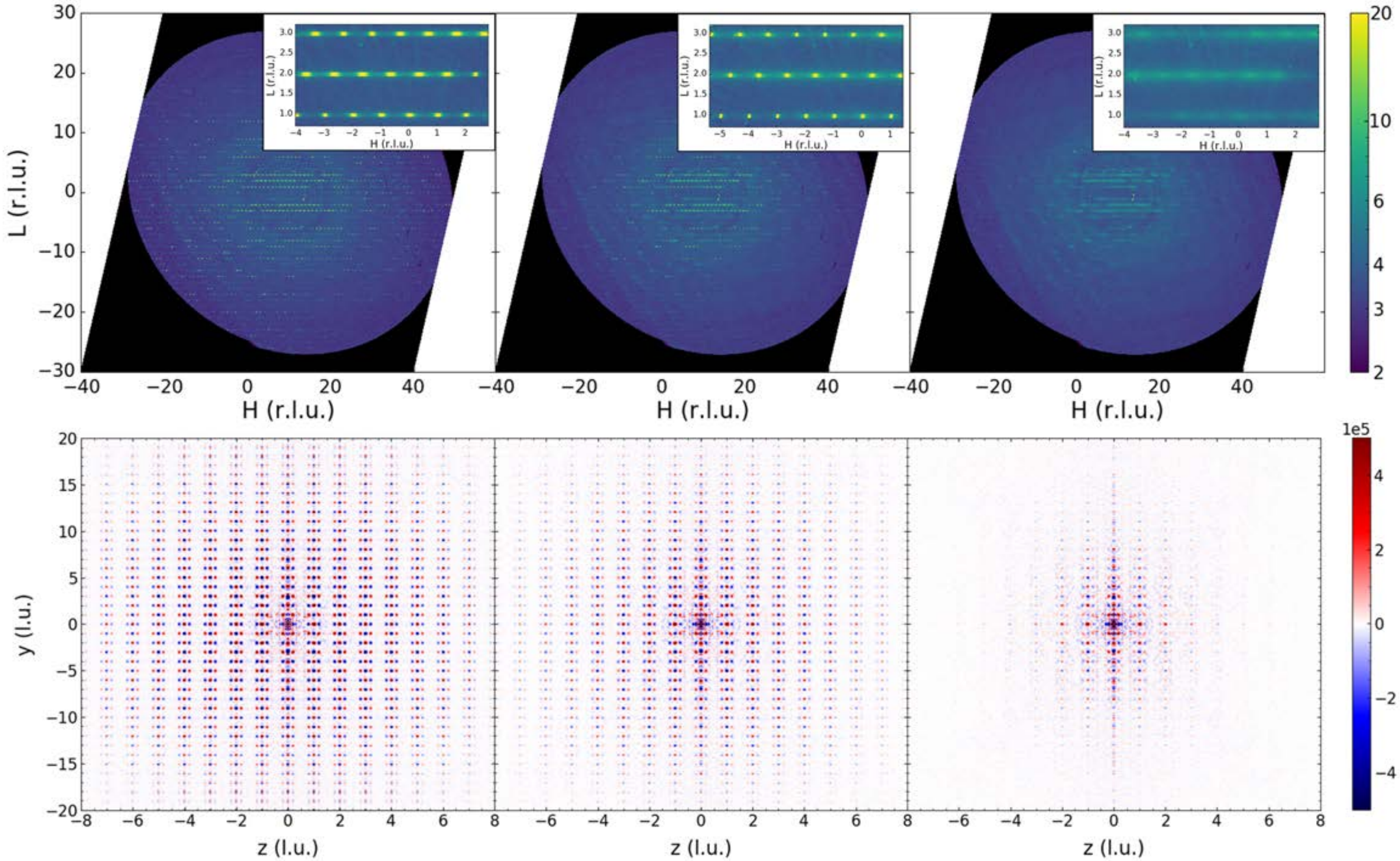

50K 150K 250K

40% Na-intercalation

3D-ΔPDF: Importance of High Energy

- Expanding the Q-range enhances the real-space resolution

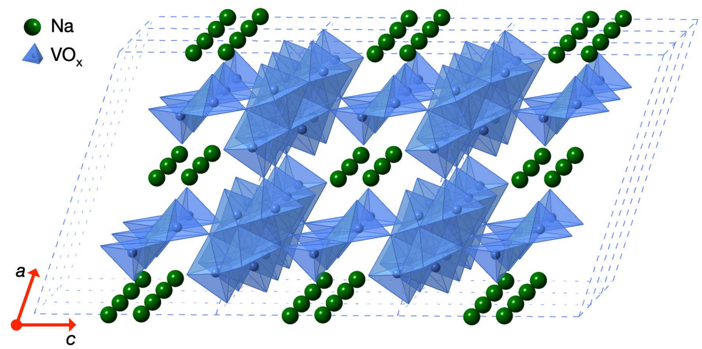

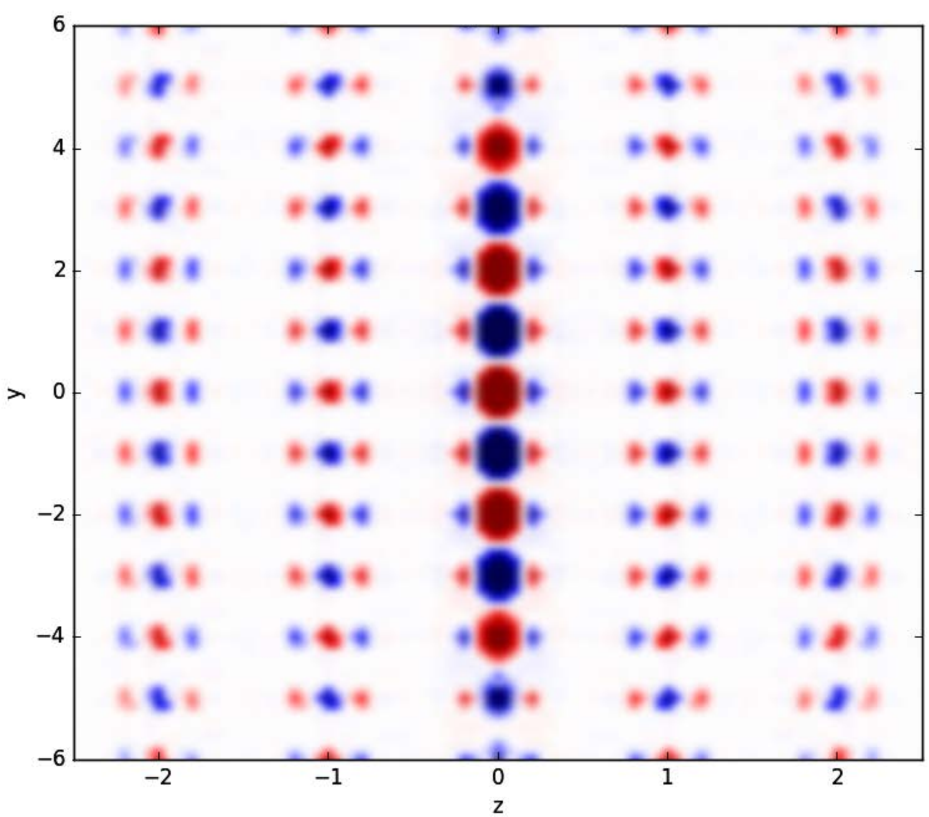

CHESS – A2 – 55keV

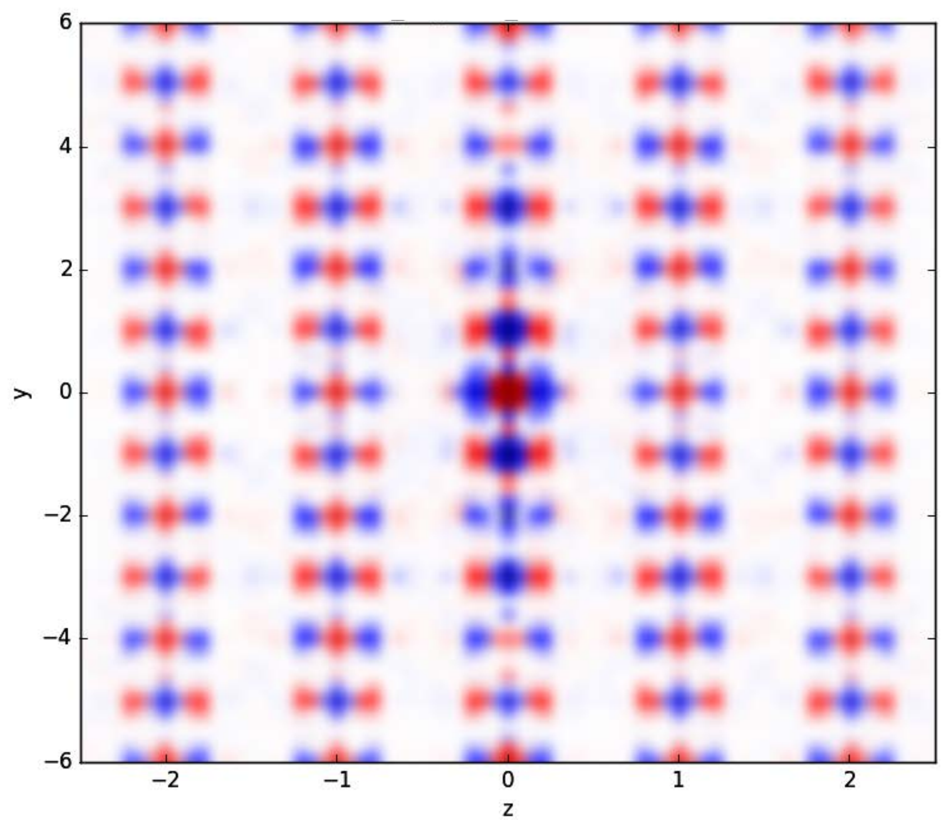

APS – 11-ID-D – 18.5keV

Back to Mullite

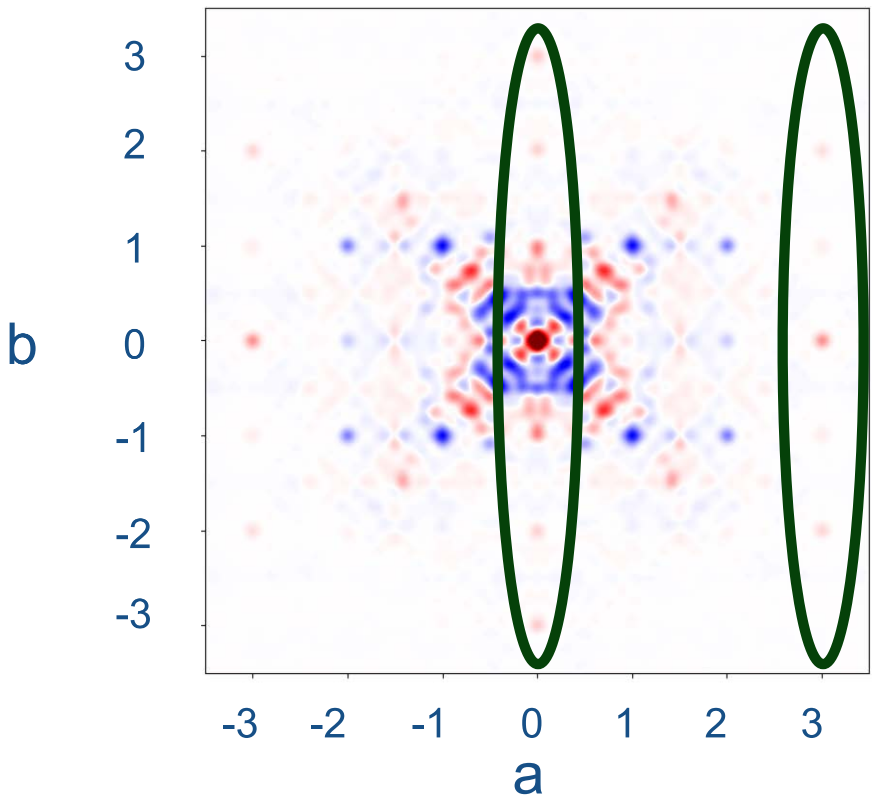

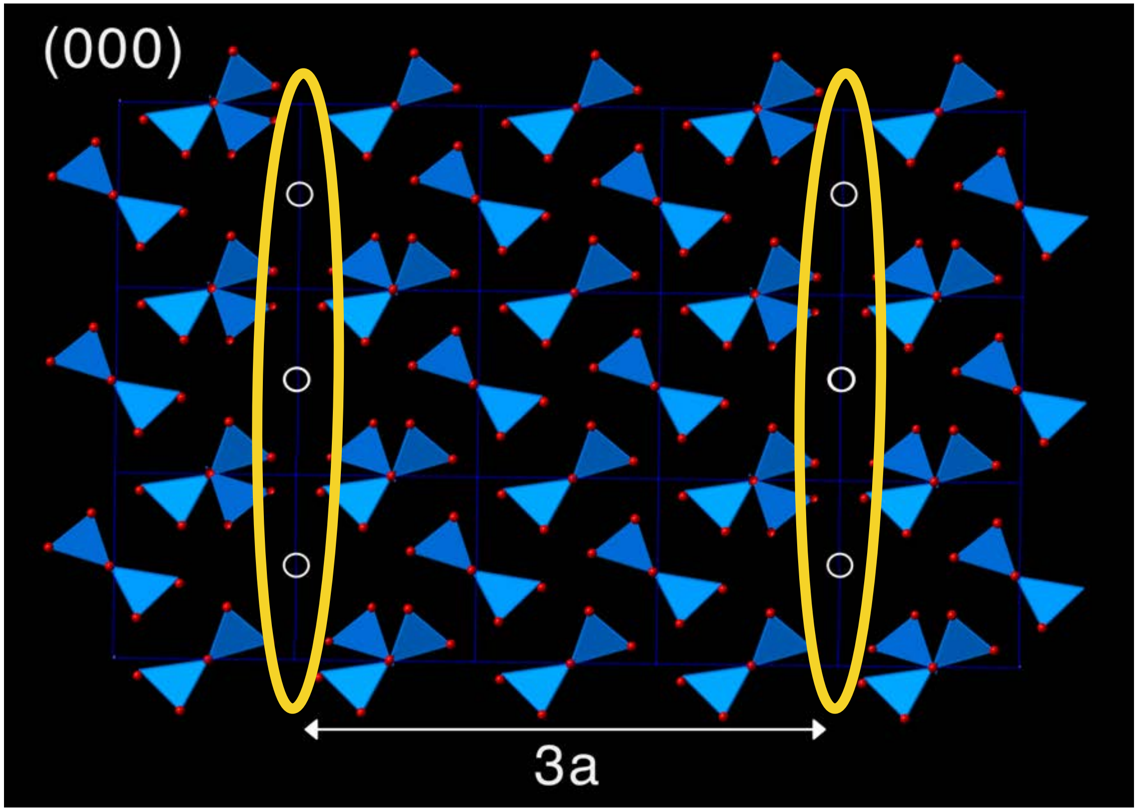

c = 0

How do I look at static disorder?

Comparison of Elastic Scattering and the Static Approximation

$$\left(\frac{d^2\sigma}{d\Omega dE'}\right)_{coh} = b_{coh}^2 \frac{k'}{k} N \frac{1}{2\pi\hbar} \int G(\vec{r},t) e^{i(\vec{Q}.\vec{r}-\omega t)} d\vec{r}.dt$$

$$\text{where } G(\vec{r},t) = \frac{1}{(2\pi)^3} \frac{1}{N} \int e^{-i\vec{Q}.\vec{r}} \sum_{j,j'} \left\langle e^{-i\vec{Q}.\vec{R}_{j'}(0)} e^{i\vec{Q}.\vec{R}_j(t)} \right\rangle$$

$$\left(\frac{d\sigma}{d\Omega}\right)_{coh}^{static} = b_{coh}^2 N \int G(\vec{r},0) e^{i\vec{Q}.\vec{r}} d\vec{r}$$

since $\hbar\delta(t) = \frac{1}{2\pi} \int_{-\infty}^{\infty} e^{i\omega t} d(\hbar\omega)$

$$\left(\frac{d\sigma}{d\Omega}\right)_{coh}^{elastic} = b_{coh}^2 N \int G(\vec{r},\infty) e^{i\vec{Q}.\vec{r}} d\vec{r}$$

- Reference: Roger Pynn, National School of Neutron and X-ray Scattering, 2018

Importance of Elastic Discrimination

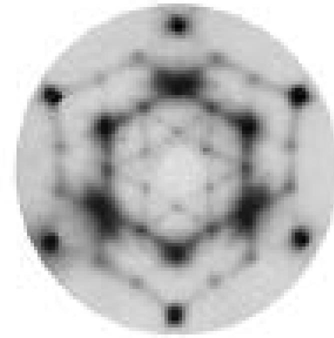

BENZIL

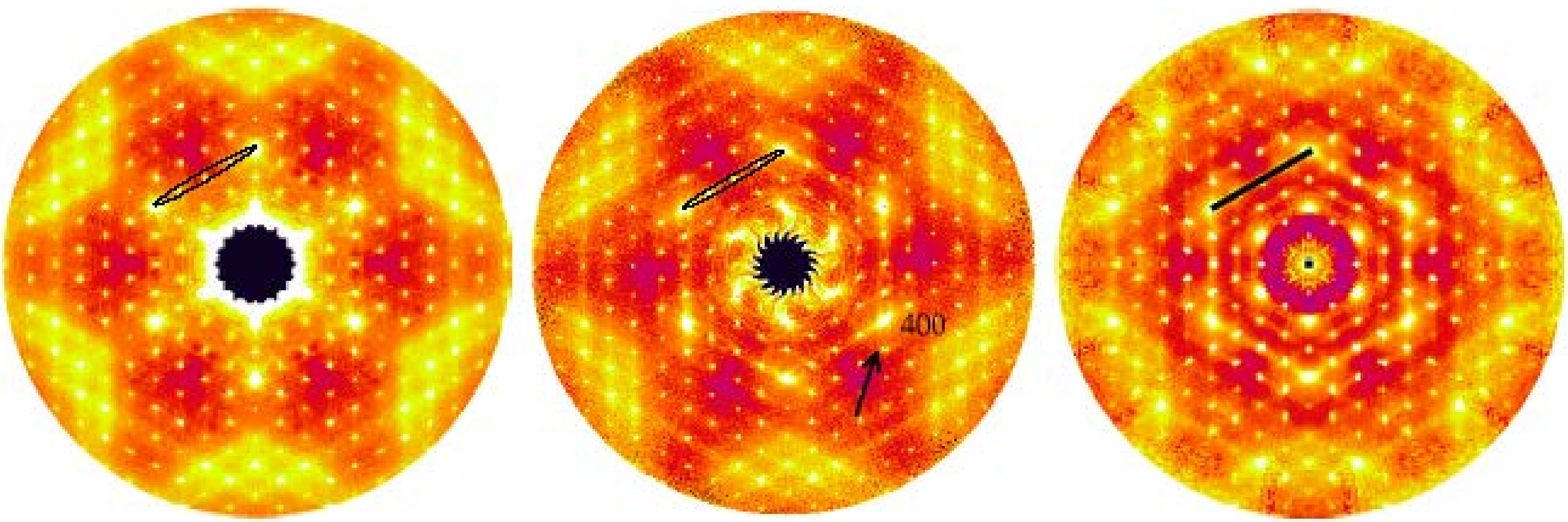

Detector 1
2θ~142.5°

Detector 2
2θ~90.0°

Detector 3
2θ~37.5°

$$Q = 4\pi\frac{sin\theta}{\lambda}$$

T. R. Welberry *et al* J. Appl. Cryst. **36**, 1400 (2003)

Measuring Large Volumes of Reciprocal Space

Conventional Time-of-Flight Neutron Methods

White Beam:
efficient

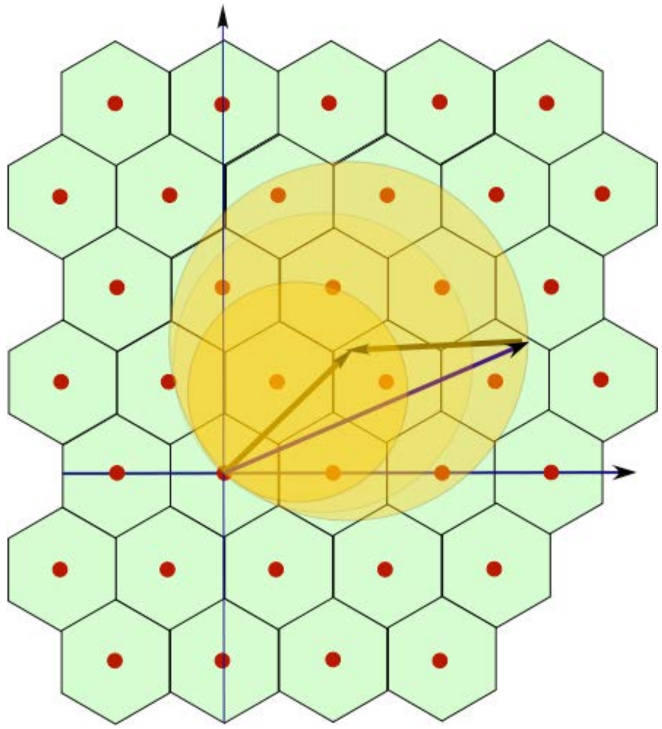

NO energy discrimination

Fixed k_i :
energy resolved

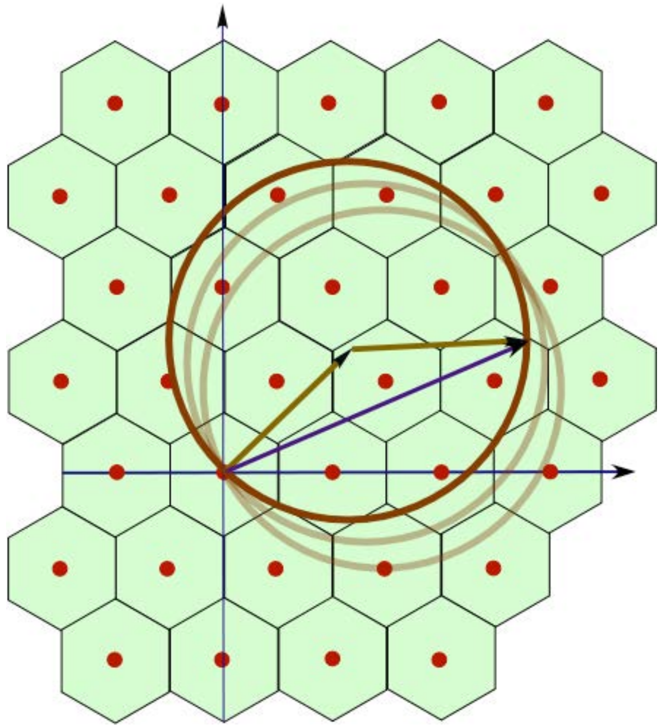

NOT efficient

Cross Correlation Chopper

TOF Laue Diffractometer

- highly efficient data collection
- wide dynamic range in Q

Statistical Chopper

- elastic energy discrimination
- optimum use of white beam

Sample with :

elastic scattering

$$\hbar\omega = 0$$

inelastic excitations

$$\hbar\omega = +E_0$$

$$\hbar\omega = -E_0$$

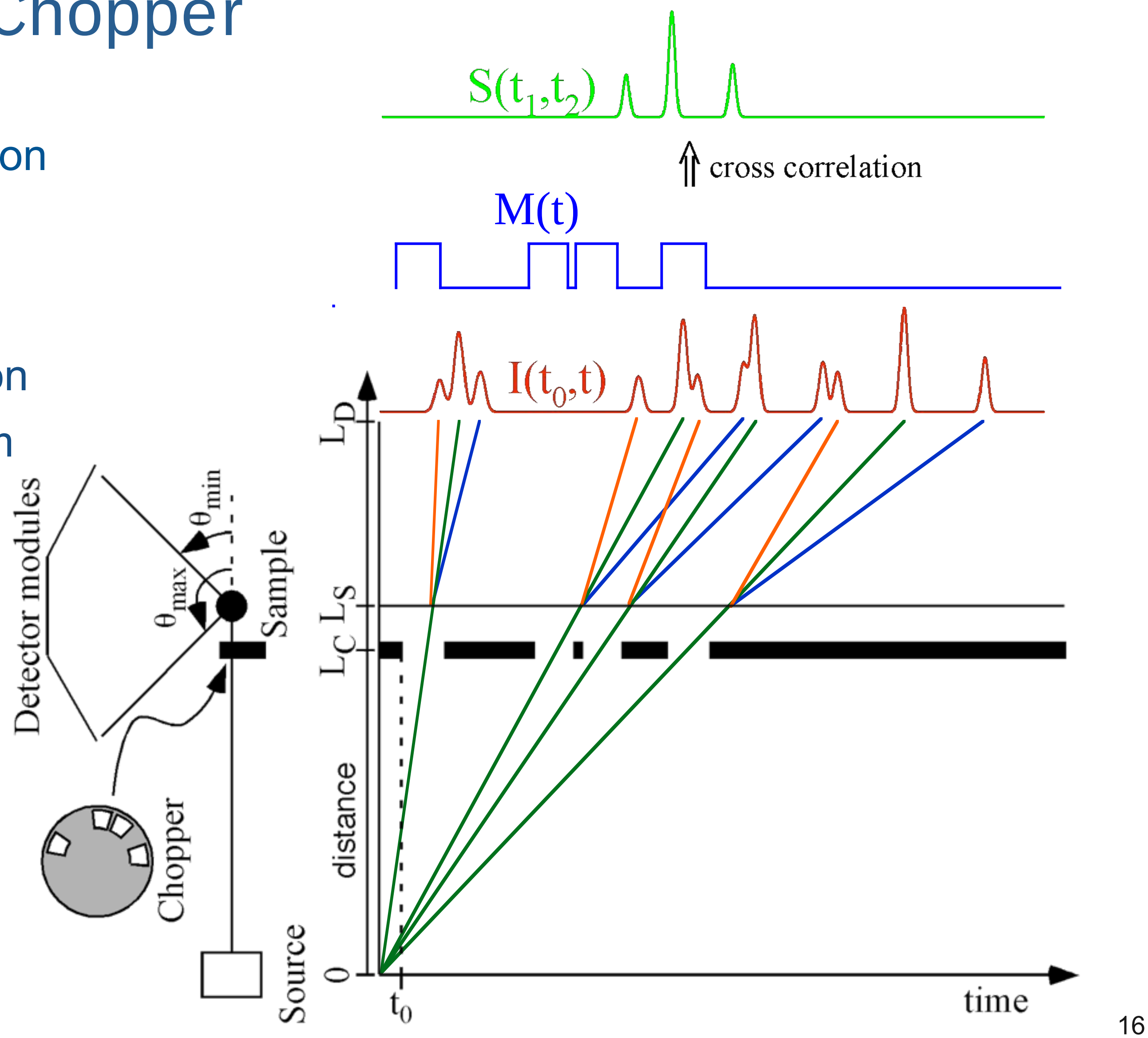

S. Rosenkranz and R. Osborn, *PRAMANA- Journal of Physics,* **71,** 705 (2008).

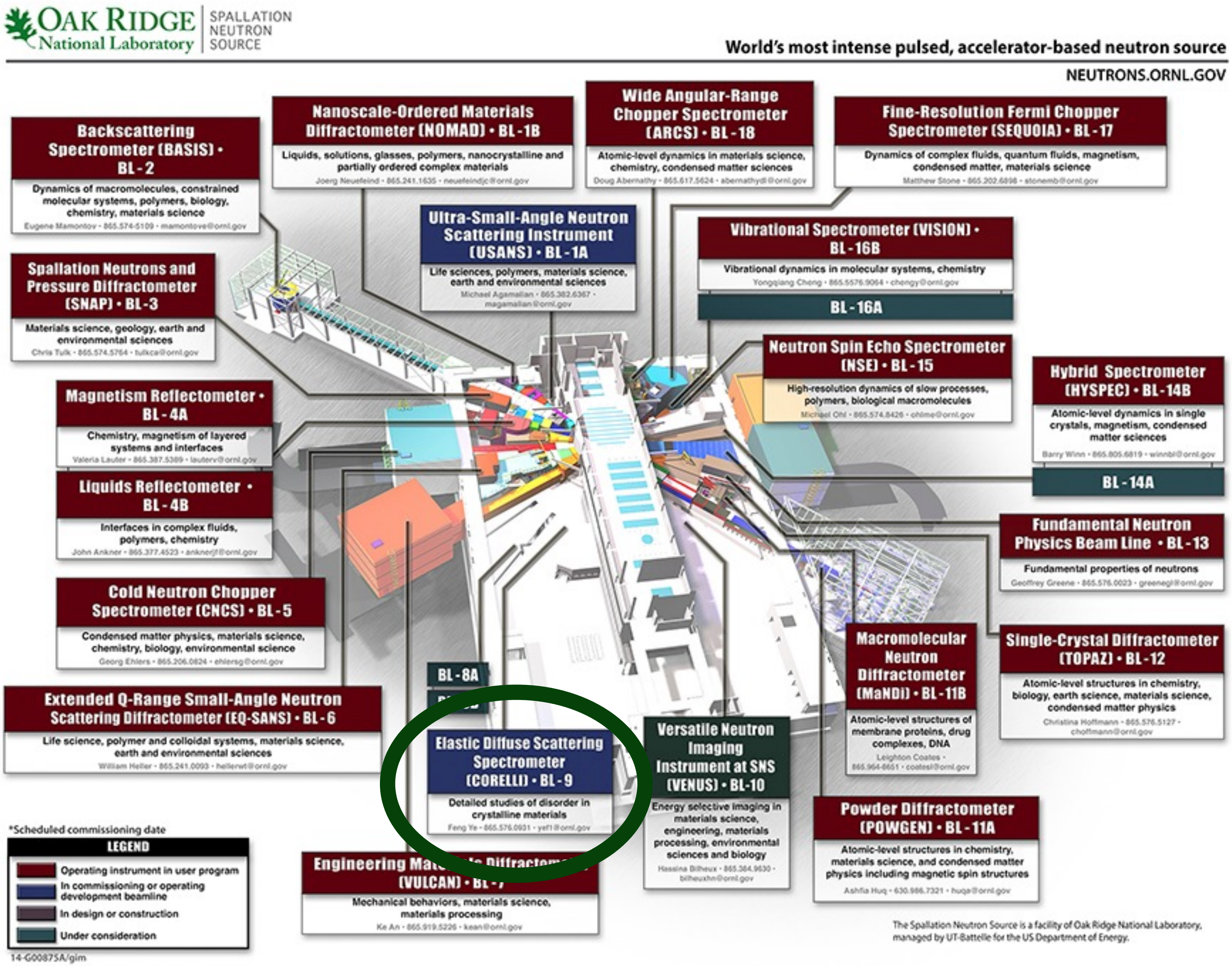
OAK RIDGE National Laboratory
SPALLATION NEUTRON SOURCE
World's most intense pulsed, accelerator-based neutron source
NEUTRONS.ORNL.GOV
Backscattering Spectrometer (BASIS) • BL-2
Dynamics of macromolecules, constrained molecular systems, polymers, biology, chemistry, materials science
Nanoscale-Ordered Materials Diffractometer (NOMAD) • BL-1B
Liquids, solutions, glasses, polymers, nanocrystalline and partially ordered complex materials
Wide Angular-Range Chopper Spectrometer (ARCS) • BL-18
Atomic-level dynamics in materials science, chemistry, condensed matter sciences
Fine-Resolution Fermi Chopper Spectrometer (SEQUOIA) • BL-17
Dynamics of complex fluids, quantum fluids, magnetism, condensed matter, materials science
Ultra-Small-Angle Neutron Scattering Instrument (USANS) • BL-1A
Life sciences, polymers, materials science, earth and environmental sciences
Vibrational Spectrometer (VISION) • BL-16B
Vibrational dynamics in molecular systems, chemistry
BL-16A
Spallation Neutrons and Pressure Diffractometer (SNAP) • BL-3
Materials science, geology, earth and environmental sciences
Neutron Spin Echo Spectrometer (NSE) • BL-15
High-resolution dynamics of slow processes, polymers, biological macromolecules
Hybrid Spectrometer (HYSPEC) • BL-14B
Atomic-level dynamics in single crystals, magnetism, condensed matter sciences
BL-14A
Magnetism Reflectometer • BL-4A
Chemistry, magnetism of layered systems and interfaces
Liquids Reflectometer • BL-4B
Interfaces in complex fluids, polymers, chemistry
Fundamental Neutron Physics Beam Line • BL-13
Fundamental properties of neutrons
Cold Neutron Chopper Spectrometer (CNCS) • BL-5
Condensed matter physics, materials science, chemistry, biology, environmental science
Macromolecular Neutron Diffractometer (MaNDi) • BL-11B
Atomic-level structures of membrane proteins, drug complexes, DNA
Single-Crystal Diffractometer (TOPAZ) • BL-12
Atomic-level structures in chemistry, biology, earth science, materials science, condensed matter physics
BL-8A
Extended Q-Range Small-Angle Neutron Scattering Diffractometer (EQ-SANS) • BL-6
Life science, polymer and colloidal systems, materials science, earth and environmental sciences
Elastic Diffuse Scattering Spectrometer (CORELLI) • BL-9
Detailed studies of disorder in crystalline materials
Versatile Neutron Imaging Instrument at SNS (VENUS) • BL-10
Energy selective imaging in materials science, engineering, materials processing, environmental sciences and biology
Powder Diffractometer (POWGEN) • BL-11A
Atomic-level structures in chemistry, materials science, and condensed matter physics including magnetic spin structures
Mechanical behaviors, materials science, materials processing
*Scheduled commissioning date
LEGEND
Operating instrument in user program
In commissioning or operating development beamline
In design or construction
Under consideration
The Spallation Neutron Source is a facility of Oak Ridge National Laboratory, managed by UT-Battelle for the US Department of Energy.
14-G00875A/gim

Corelli

Instrument Scientists
Feng Ye
Yaohua Liu

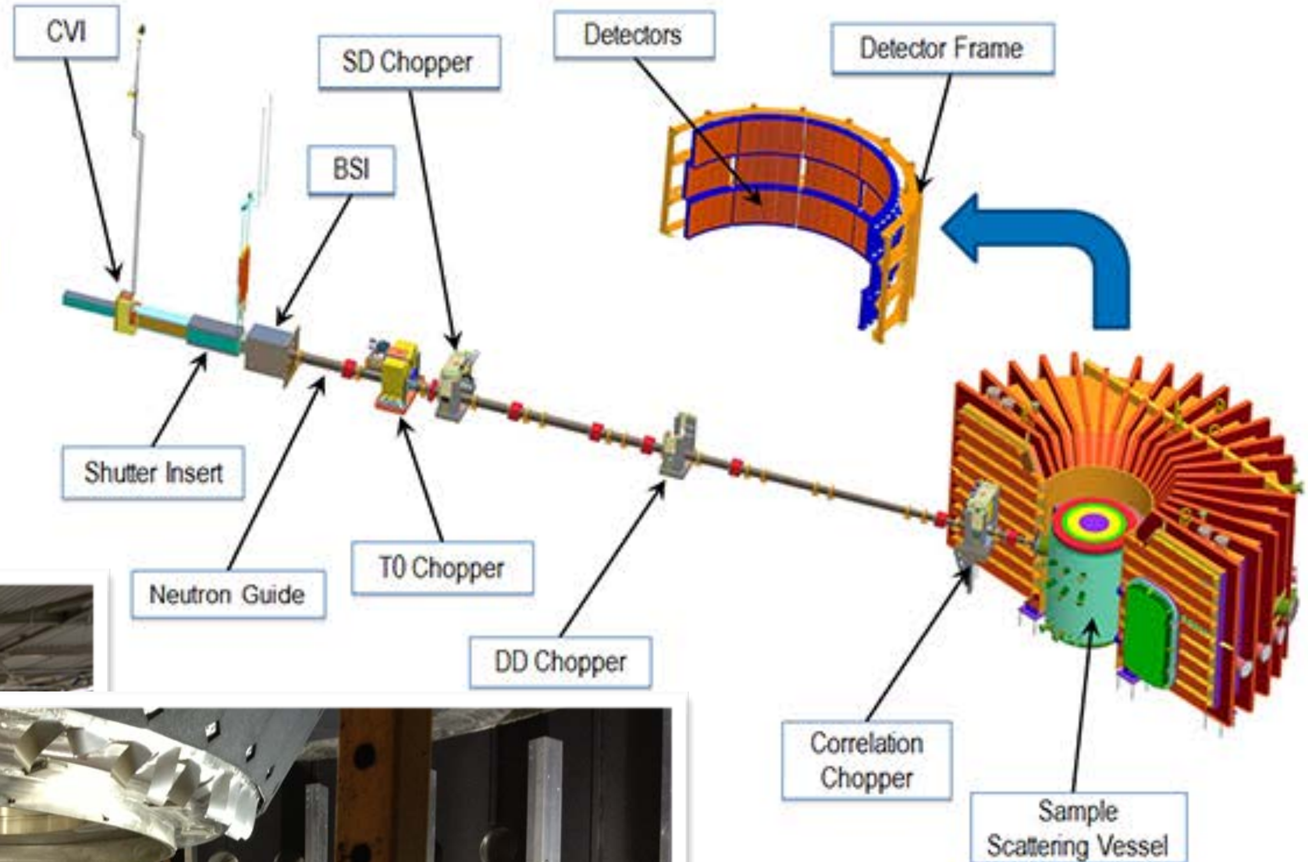

Instrument Proposers
Stephan Rosenkranz
Ray Osborn

Cross Correlation in Action

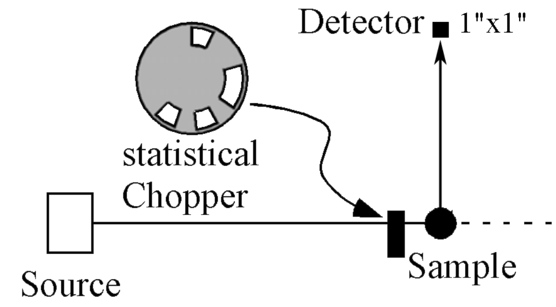

Before cross-correlation

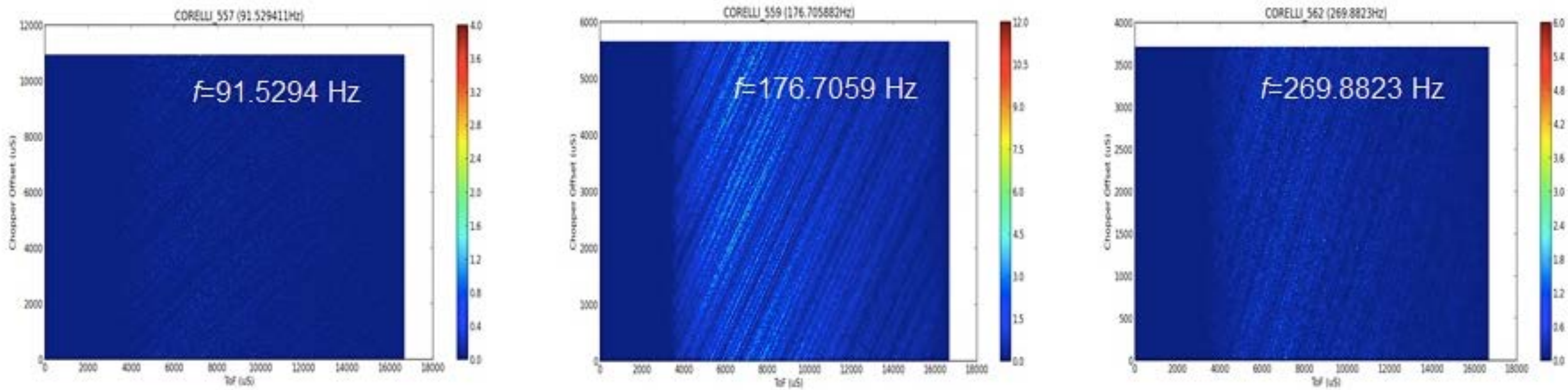

After cross-correlation

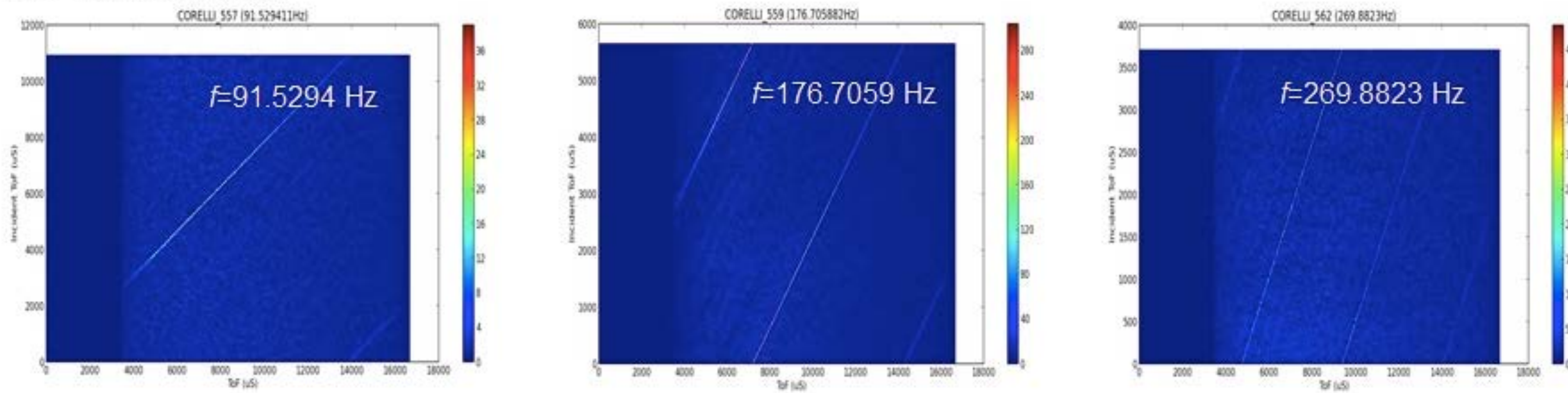

Elastic Discrimination with Cross Correlation

Benzil $C_{14}H_{10}O_2$

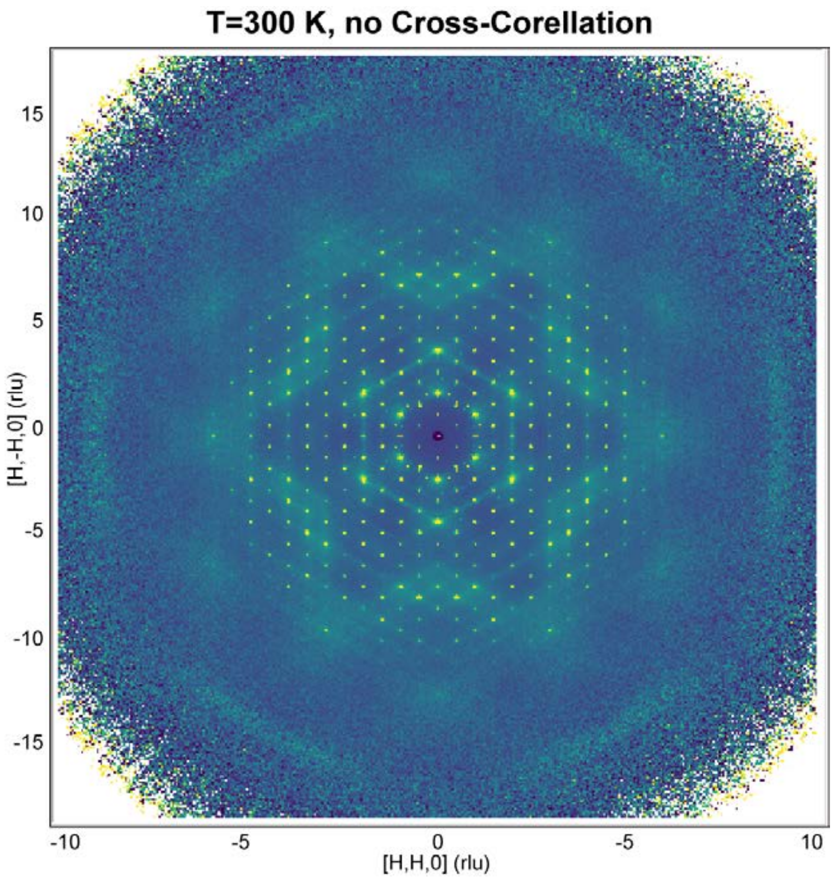

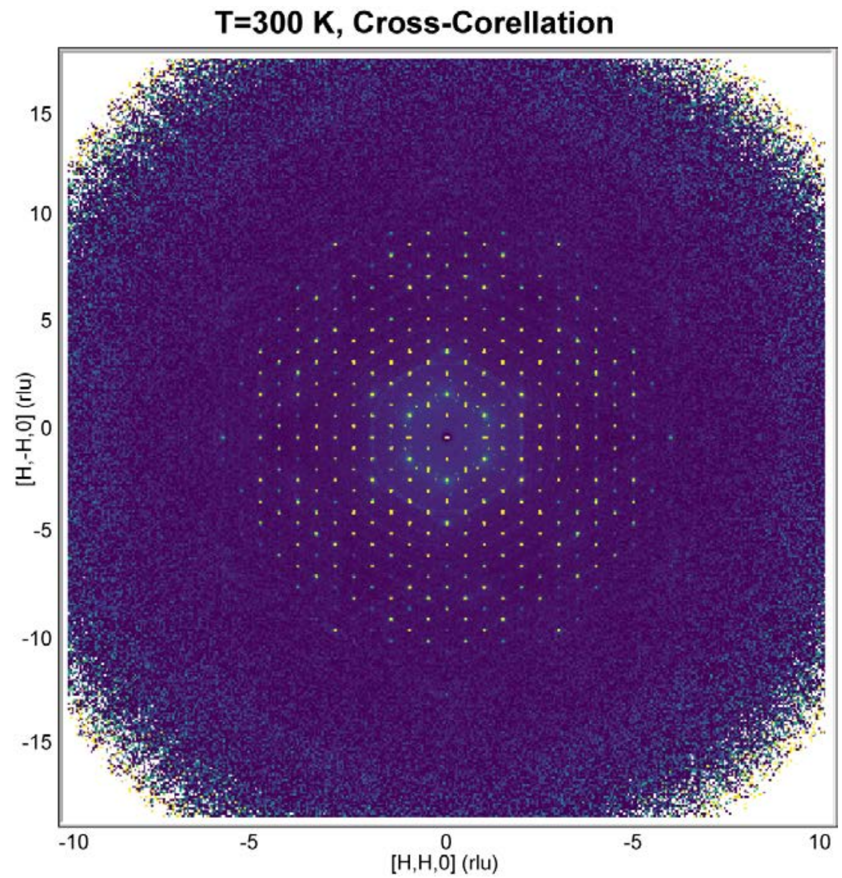

T. R. Welberry and R. Whitfield, Quantum Beam Science **2**, 2 (2018)

Relaxor Ferroelectrics - $Pb(Mg_{1/3}Nb_{2/3})O_3$-$xPbTiO_3$

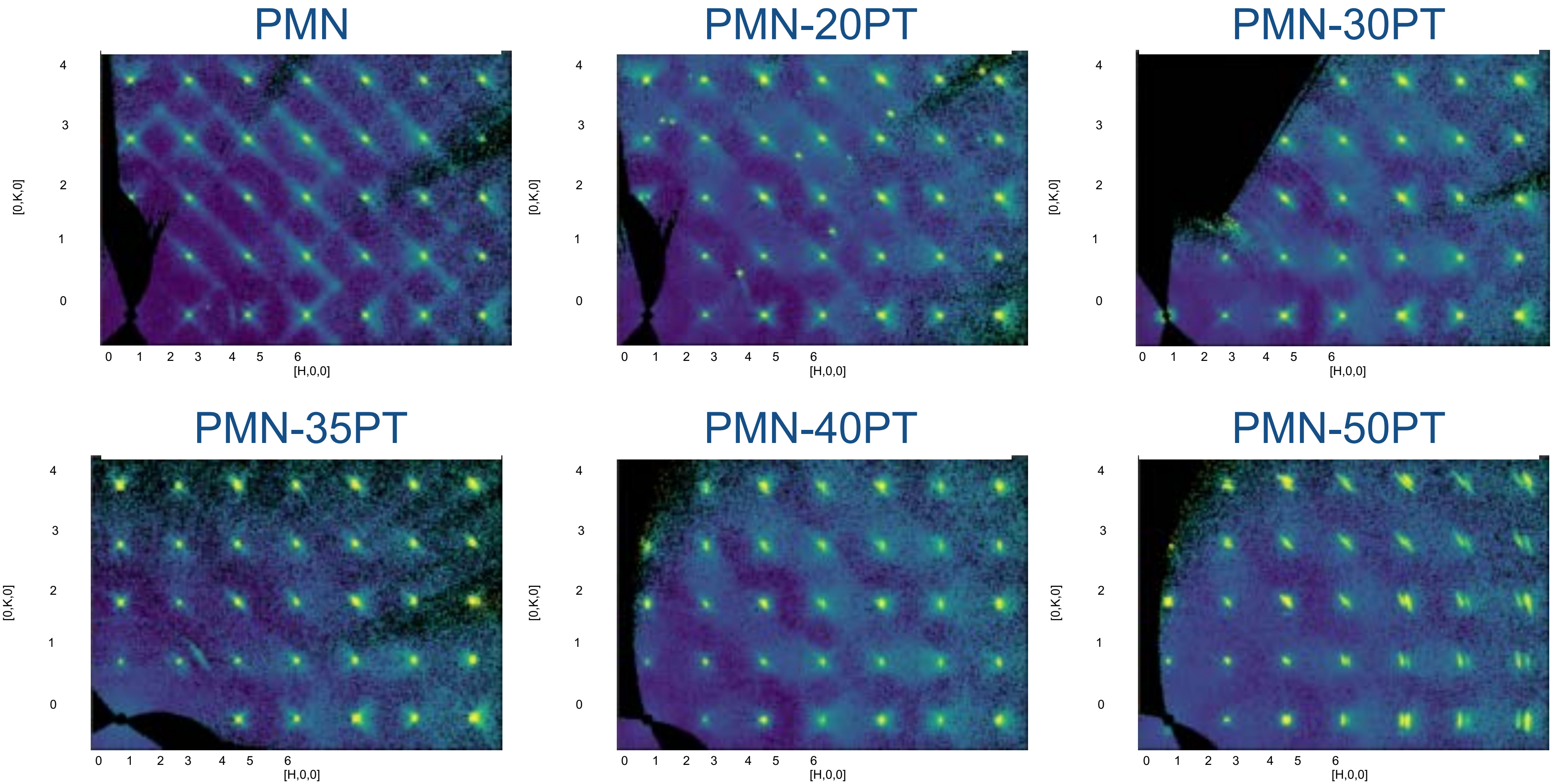

M. J. Krogstad, P. M. Gehring, S. Rosenkranz, R. Osborn, F. Ye, Y. Liu, J. P. C. Ruff, W. Chen, J. M. Wozniak, H. Luo, O. Chmaissem, Z.-G. Ye, and D. Phelan, Nat Mater **48**, 1 (2018).

Complementarity of Neutrons and X-rays

$Pb(Mg_{1/3}Nb_{2/3})O_3$-30%$PbTiO_3$

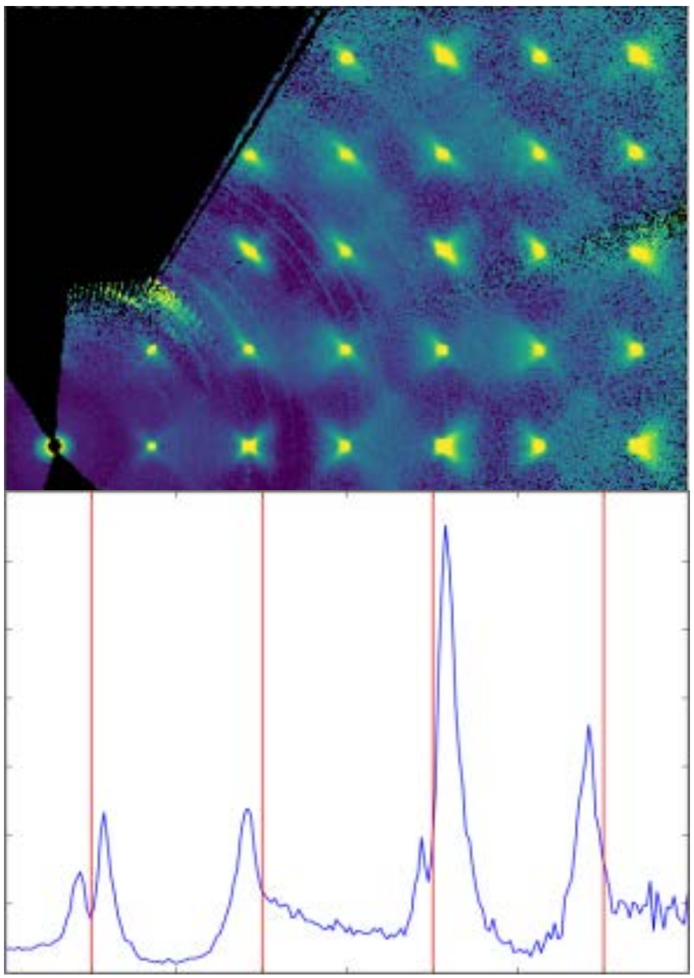

Corelli Neutrons

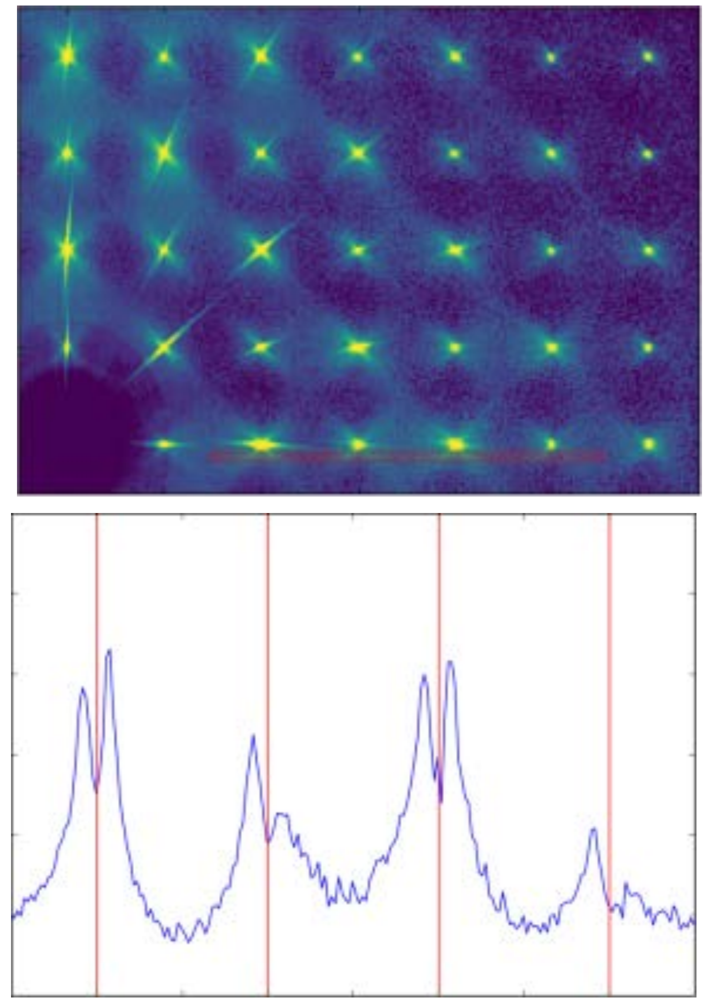

CHESS 55keV X-rays

Sublattice Melting in Superionic $Cu_{1.8}Se$

- It has been proposed that $Cu_{2-x}Se$ is a Phonon Liquid-Electron Crystal thermoelectric
  - zT > 1.5 at high temperature

LETTERS
PUBLISHED ONLINE: 11 MARCH 2012 | DOI: 10.1038/NMAT3273
nature materials

Copper ion liquid-like thermoelectrics

Huili Liu[1,2], Xun Shi[1,3]*, Fangfang Xu[3], Linlin Zhang[3], Wenqing Zhang[3], Lidong Chen[1]*, Qiang Li[4], Ctirad Uher[5], Tristan Day[6] and G. Jeffrey Snyder[6]

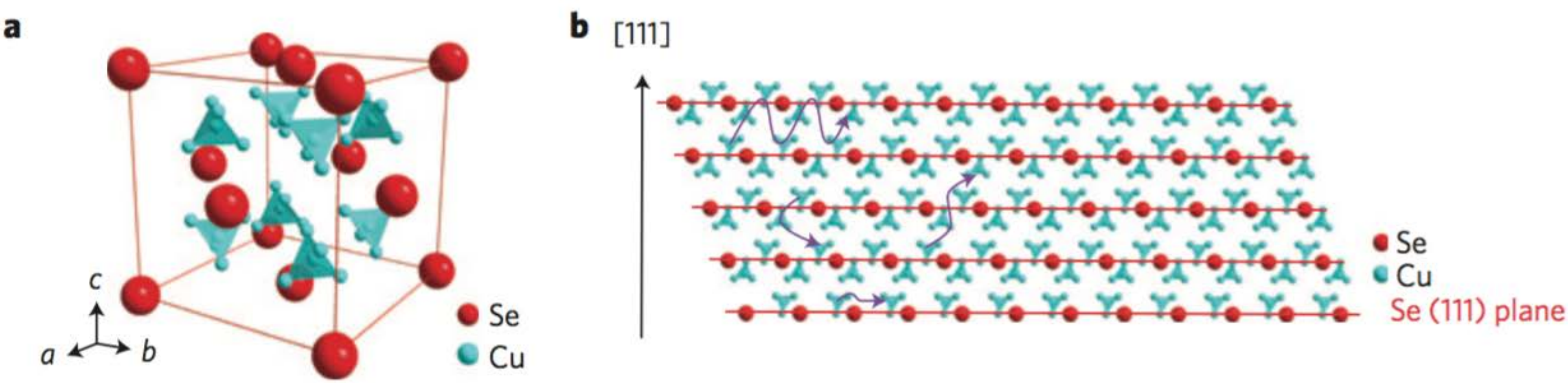

3D-ΔPDF from $Cu_{1.8}Se$

Corelli Data

Alex Rettie

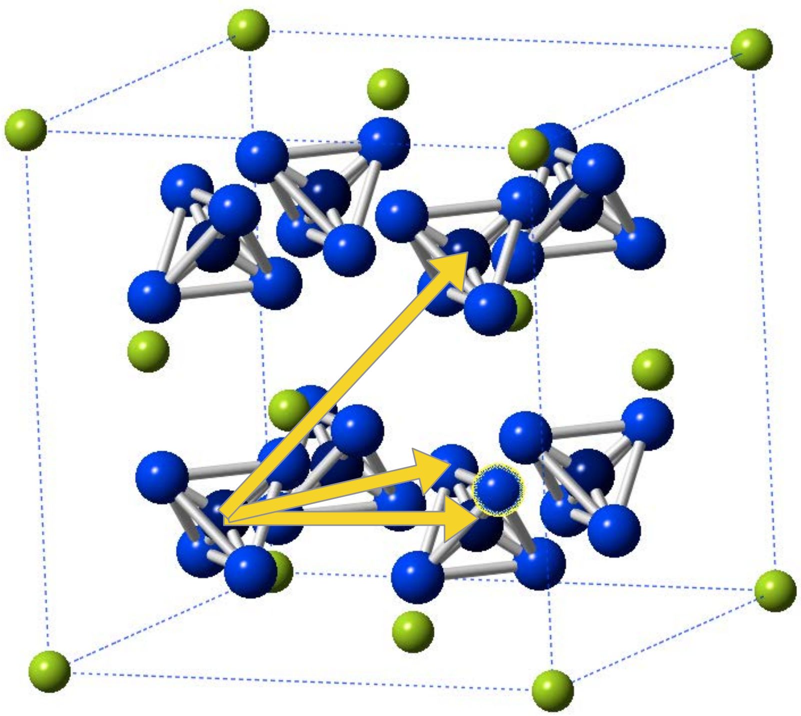

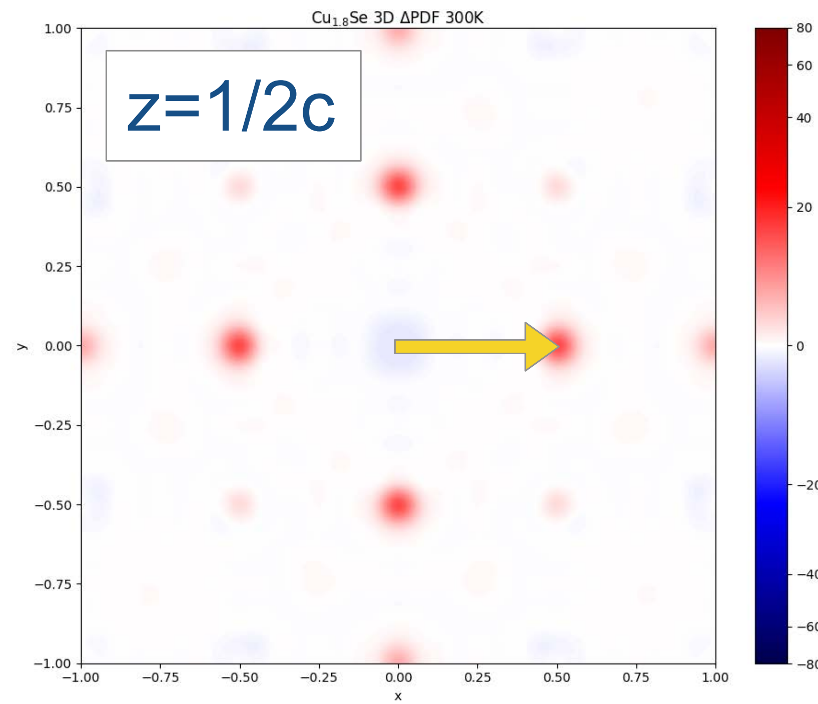

Qh

Symmetrized Corelli Data

The Future

- High-Energy X-rays
  - Absorption lengths similar to neutrons
  - Detectors now have sensors optimized for high energies, *e.g.* Pilatus 2M CdTe
- Micro-diffuse scattering
  - Benefiting from increased brightness of, *e.g.,* APS Upgrade
- Increasing use of *ab initio* computational modeling
  - Allowing more complex systems to be investigated
  - Less dependence on intuition in modeling
- Enhanced analysis tools
  - Machine learning
  - Correlated data analysis
  - Easier co-refinement of neutrons and x-rays

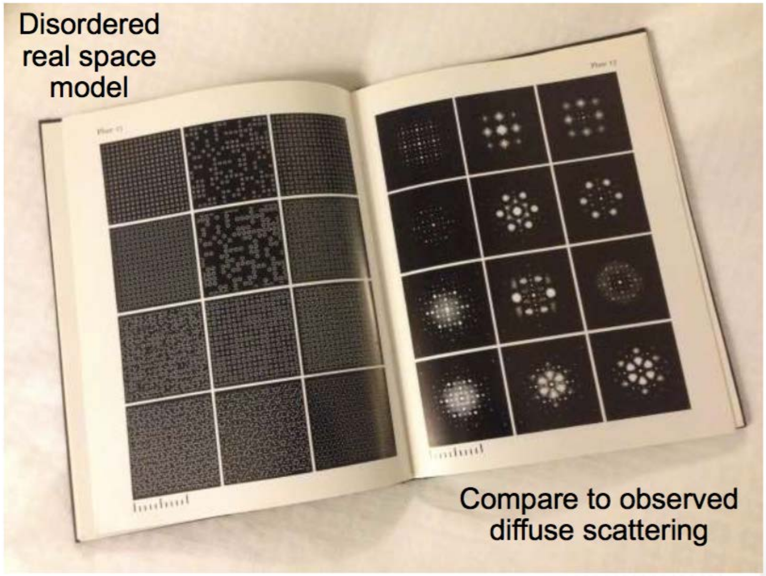

Atlas of Optical Transforms, Harburn, Taylor and Welberry (1975)

A Few References

- T. R. Welberry & B. Butler, Chem Rev **95**, 2369–2403 (1995).
- F. Frey, Acta Cryst B **51**, 592–603 (1995).
- T. R. Welberry & D. J. Goossens, Acta Cryst A **64**, 23–32 (2007).
- D. A. Keen & A. L. Goodwin, Nature News **521**, 303–309 (2015).

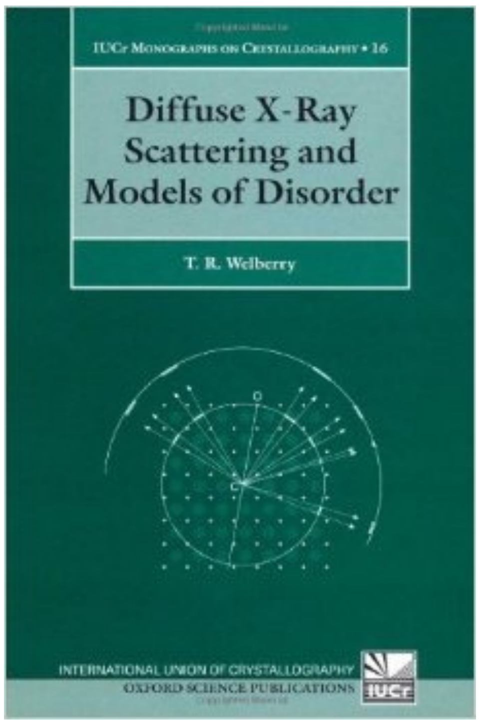

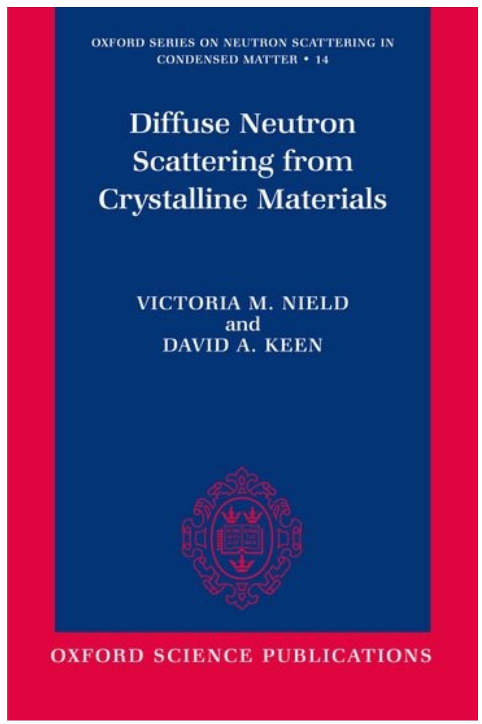

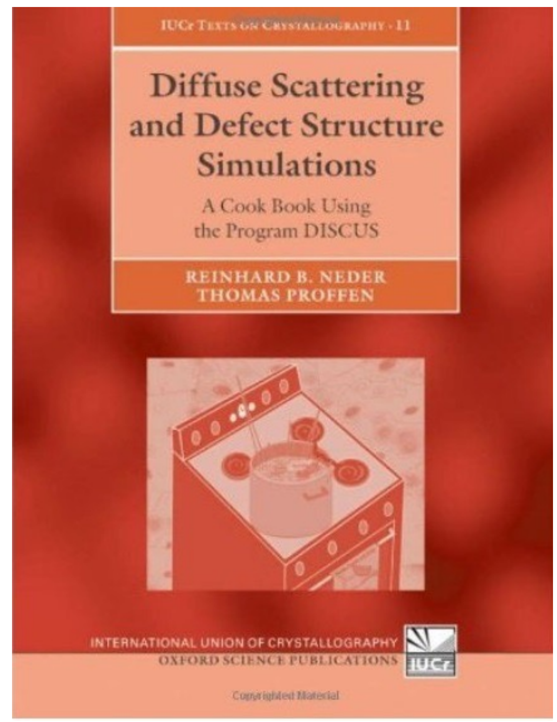

Diffuse Scattering Song

- Come eager young scholars - so tender and new
  I'll teach you diffraction - what I says mostly true
  Between the Bragg Peaks lies a world where you see
  Fluctuations and defects- they stand out plane-ly
- *Chorus*
  For its dark as a dungeon between the Bragg peaks
  But here in the darkness - each defect speaks
  It gathers- from throughout- reciprocal space
  And re-distributes all over the place.
- Between the Bragg peaks - one thing that we see
  Is TDS on our CCD
  Intensity totals are conserved- you can't win
  It steals from the Bragg peaks that stay very thin
- Substitutional alloys can cause quite a stir
  The shorter the length scale the greater the blur
  With care you can find out the bond length between
  Each atom pair type-the measurements clean
- Dislocations and other- type 2 defects
  Destroy the Bragg peaks -they turn them to wrecks
  But near the Bragg peaks- you still can see
  Intense diffraction continuously
- Many -are- the defects you find
  Between the Bragg peaks where others are blind
  So go tell your friends and impress your boss
  You've new understanding -with one hours loss

Gene Ice

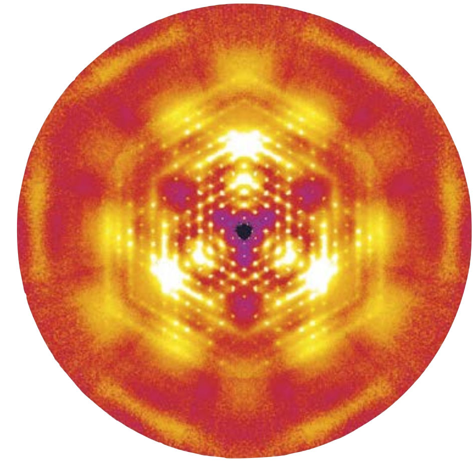

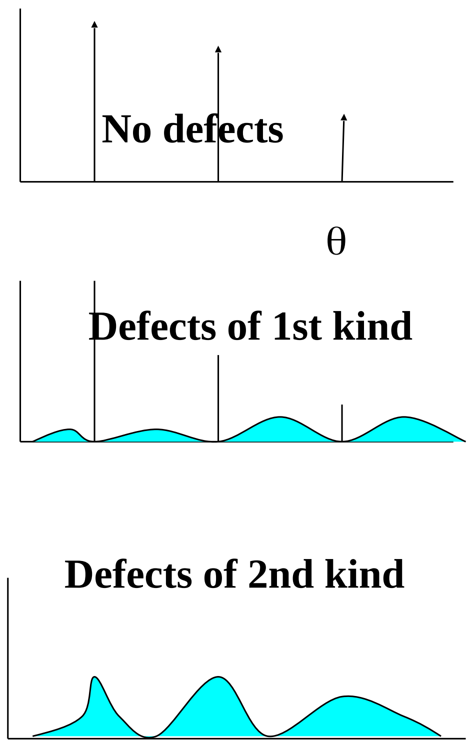

Krivoglaz Classifications